Passive Acoustic Bearing Estimation Algorithms Applied on Hydro Acoustic Data

HÅKAN SELHAMMER

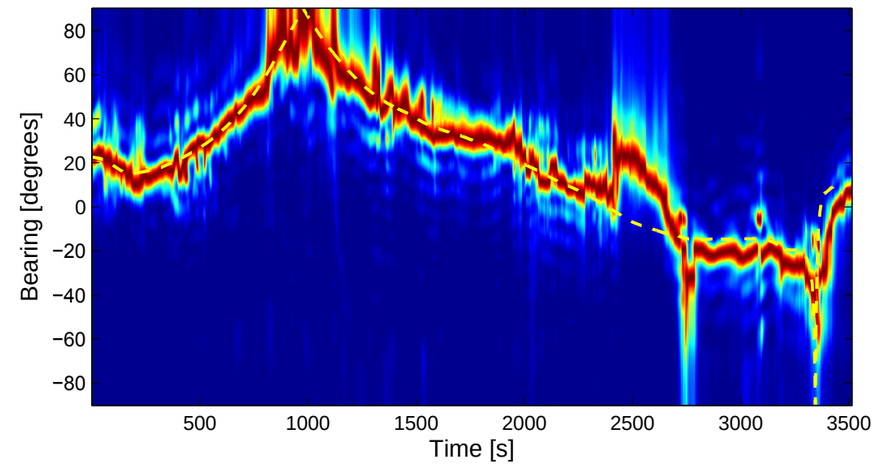

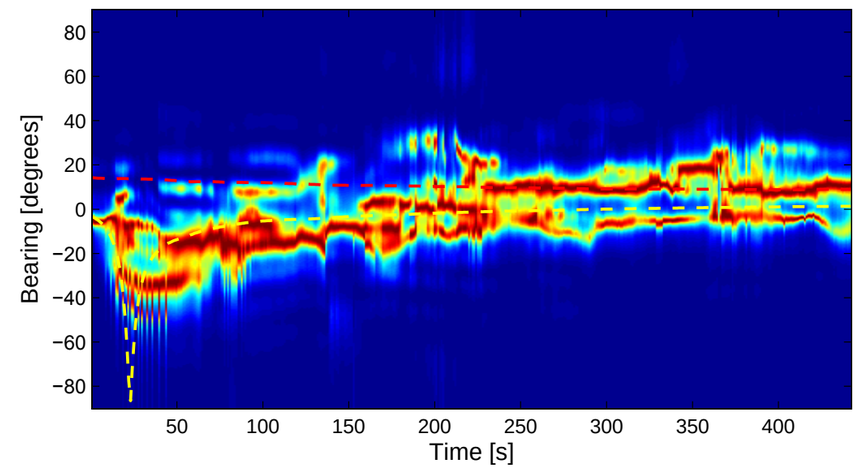

FOI is an assignment-based authority under the Ministry of Defence. The core activities are research, method and technology development, as well as studies for the use of defence and security. The organization employs around 1350 people of whom around 950 are researchers. This makes FOI the largest research institute in Sweden. FOI provides its customers with leading expertise in a large number of fields such as security-policy studies and analyses in defence and security, assessment of different types of threats, systems for control and management of crises, protection against and management of hazardous substances, IT-security an the potential of new sensors.

FOI
Defence Research Agency
Systems Technology
SE-164 90 Stockholm

Phone: +46 8 555 030 00
Fax: +46 8 555 031 00

www.foi.se

FOI-R-- 1923 --SE Technical report
ISSN 1650-1942 February 2006

Systems Technology

Håkan Selhammer

Passive Acoustic Bearing Estimation Algorithms Applied on Hydro Acoustic Data

FOI-R-- 1923 --SE Technical report Systems Technology
ISSN 1650-1942 February 2006

Issuing organization	Report number, ISRN	Report type
FOI – Swedish Defence Research Agency Systems Technology SE-164 90 Stockholm	FOI-R -- 1923 --SE	Technical report
	Research area code 4. C4ISTAR	
	Month year February 2006	**Project no.** E60702
	Sub area code 43 Underwater Surveillance, Target acquistion and Reconnaissance	
	Sub area code 2	

Author/s (editor/s)	Project manager
Håkan Selhammer	Eva Dalberg
	Approved by Monica Dahlén
	Sponsoring agency Swedish Armed Forces
	Scientifically and technically responsible Magnus Lundberg

Report title

Passive Acoustic Bearing Estimation Algorithms Applied on Hydro Acoustic Data

Abstract

This thesis evaluates the bearing performance of three different bearing estimation algorithms in a real application, where the target is a moving surface vessel. The evaluated methods are Conventional Beamforming and two high-resolution estimators Minimum Variance and MUSIC (MUltiple SIgnal Classification). The spatial covariance matrix is of great importance to obtain accurate bearing estimates in all three estimators, which means that it has to be well estimated.

The condition of the spatial covariance matrix and the performance of the bearing estimators have been studied regarding the length of the estimation window (i.e. number of samples used for each bearing estimate) and recursive updating of the spatial covariance matrix. This has been performed by first detecting the target, and then tracking it during the entire recording.

From measurements it has been shown that recursive updating of the spatial covariance matrix yields better bearing performance than using longer estimation windows. In addition, the computational time and the time delay is reduced. Both Conventional Beamforming and MUSIC yield a very accurate bearing performance, which is substantially better than the Minimum Variance estimator. The MUSIC method shows the best resolution properties and is able to separate two closely spaced sources.

Keywords

Bearing estimation, hydro acoustic, Conventional Beamforming, CB, Minimum Variance, MV, MUSIC, Recursive Updating

Further bibliographic information	Language English
ISSN 1650-1942	**Pages** 60 p.
	Price acc. to pricelist

Utgivare FOI - Totalförsvarets forskningsinstitut Systemteknik 164 90 Stockholm	**Rapportnummer, ISRN** FOI-R-- 1923 --SE	**Klassificering** Teknisk rapport
	Forskningsområde 4. Ledning, informationsteknik och sensorer	
	Månad, år Februari 2006	**Projektnummer** E60702
	Delområde 43 Undervattenssensorer	
	Delområde 2	
Författare/redaktör Håkan Selhammer	**Projektledare** Eva Dalberg	
	Godkänd av Monica Dahlén	
	Uppdragsgivare/kundbeteckning Försvarsmakten	
	Tekniskt och/eller vetenskapligt ansvarig Magnus Lundberg	

Rapportens titel

Passiva akustiska riktningsbestämningstekniker tillämpade på hydroakustiska mätdata

Sammanfattning

Syftet med detta examensarbete är att utvärdera bäringsprestandan hos tre olika metoder mot inspelad data från en verklig sonarapplikation, där källan är ett fartyg i rörelse. De utvärderade metoderna är klassisk lobformning och två högupplösande metoder Minimum Variance och MUSIC (MUltiple SIgnal Classification). Den spatiala kovariansmatrisen har en central betydelse för noggrannheten i bäringsestimaten för alla tre metoderna, vilket gör att den måste vara välestimerad.

Estimeringen av den spatiala kovariansmatrisen och bäringsmetodernas prestanda har utvärderats med avseende på längden hos estimeringsfönstret (d.v.s. antal använda sampel för varje bäringsestimat) och rekursiv uppdatering av den spatiala kovariansmatrisen). Detta har gjorts genom att först etablera ett målspår och sedan följa detta under hela inspelningen.

Mätningarna har visat att den rekursiva uppdateringen av den spatiala kovariansmatrisen ger en bättre bärings-prestanda än att använda längre estimeringsfönster. Dessutom kommer beräkningstiden och eftersläpningen i bäringsestimaten att reduceras. Både klassisk lobformning och MUSIC ger väldigt noggranna bäringsprestanda, till skillnad från Minimum Variance vilken har en betydligt sämre noggrannhet. MUSIC metoden är dock den metod som visar på de bästa upplösningsegenskaperna och har visat sig vara kapabel att separera två närliggande mål.

Nyckelord

Bäringsestimering, hydroakustisk, klassisk lobformning, CB, Minimum Varians, MV, MUSIC, Rekursiv Updatering

Övriga bibliografiska uppgifter	**Språk** Engelska
ISSN 1650-1942	**Antal sidor:** 60 s.
Distribution enligt missiv	**Pris: Enligt prislista**

Contents

1 Abbreviations and Symbols

bias	Average deviation from true value
Broad Side	The source is located at the normal of the array
CB	Conventional Beamforming
dB	Decibel
DOA	Direction Of Arrival
End Fire	The source is located at the extension direction of the array
EV	EigenVector method
FFT	Fast Fourier Transform
Hz	Hertz
MATLAB	MATrix LABoratory
MaxPM	Maximum Peak Method
MDL	Minimum Description Length
MeanPM	Mean Power Method
MV	Minimum Variance method
MUSIC	MUltiple SIgnal Classification
PSD	Power Spectral Density
RMS	Root Mean Square
SCM	Spatial Covariance Matrix
SFM	Single Frequency Method
SONAR	SOund NAvigation and Ranging
SNR	Signal-to-Noise Ratio
STD	STandard Deviation
ULA	Uniform Linear Array

x	Time domain signal
$\mathbf{x}$	Time domain snapshot vector
X	Frequency domain signal
$\mathbf{X}$	Frequency domain snapshot vector
$\mathbf{S}$	Steering vector
$\mathbf{R}$	Spatial Covariance Matrix
$\mathbf{P}$	Power
X^H	Hermitian transpose of X

M	Number of sensors
N	Number of snapshots
f	Frequency
f_s	Sampling Frequency
c	Propagation speed in water
d	Distance between sensors
α	Recursive updating constant
θ	Pointing direction/Bearing
λ	Wavelength

2 Introduction

Sonar (SOund NAvigation and Ranging) is a well established technique for mapping and finding underwater objects. It can be used in many different situations such as submarine and mine detection, bathymetry measurements (echo sounding), commercial fishing, diving safety, underwater communication. One of the most important areas is the Direction Of Arrival (DOA) estimation of sound-emitting sources. Sound waves are acoustic waves and is wave propagation by particle movements, often with less attenuation than electro magnetic waves, e.g. radio and light waves.

2.1 Background

Underwater surveillance systems for detection and localization of surface ships and submarines have been a major research area for the last decades, at many defence agencies, including the Swedish Defence Research Agency FOI. The substantial growth in performance of digital systems during the past years has made it possible to use more complex computing algorithms to meet the demand of higher precision and more robust systems. Several studies have been performed in this area, and many studies (reports and articles) describing different kinds of methods, with varying order of complexity, to estimate the bearing and range of sources.

A surveillance system can be passive or active. The advantage of a passive system is the ability of getting source information without exposing the presence and location of your own sonar platform.

The most common method of DOA estimation is called Conventional Beamforming (CB). CB and most other DOA algorithms use the Spatial Covariance Matrix (SCM) for the bearing estimation. Therefore, in order to get a numerically good estimate of the bearing with as small errors as possible, the covariance matrix has to be well estimated for all sensor combinations.

One major drawback with CB is the limited resolution capability (i.e. the ability to resolve two closely spaced sources) due to the aperture of the array. Therefore, it has been necessary to find other methods that address the issue of higher resolution. The methods studied in this report are MV (Minimum Variance) and MUSIC (MUltiple SIgnal Classification), both with higher degree of complexity and better resolution performance than CB.

The performance of the bearing algorithms in a real application will be studied by first finding the present source, and then track it during the entire recording. This will be done by searching the direction with the maximum power, which should be related to the power of the source. Sometimes multipath propagation or other disturbances can cause large errors in the bearing estimation. How to deal with such error sources is not addressed in this thesis.

2.2 Issues

The following issues are addressed in this thesis:

- Finding an appropriate length of the estimation window, with respect to the number of snapshots, in order to obtain well estimated covariance matrices.
- Recursive updating of SCM will be investigated. This updating can be performed dependent on, e.g. the SNR level of the received signal.
- The performance of three different direction estimating methods (CB, MV, MUSIC) are evaluated with real sonar data.

- The algorithms for the bearing estimation have been implemented in Matlab. This is done in a user friendly and flexible way allowing different measuring conditions, e.g. with different number of sensors and distance between adjacent sensors.

2.3 Model Discussion

The sensor array that is considered in this thesis is a passive linear sensor array consisting of M identical omni-directional sensors, which are equally spaced along the array.

2.3.1 Data Model

Assume that there is a radiating source located in the far-field of the array. The source emits a signal that is assumed to be a narrowband signal or harmonically decomposed, which can be expressed as

$$s(t) = u(t)\cos(2\pi f t + \phi(t)) \tag{1}$$

where f is the frequency, $u(t)$ is the amplitude and $\phi(t)$ is the phase. The source location, i.e. the Direction Of Arrival (DOA) θ (with regard to the array aperture), will yield different time delays τ_m at the M sensors in the array relative a reference sensor (see Figure 2 in Chapter 3). The signal that is received at the mth sensor in the array can be expressed as

$$x_m(t) = h_m(t) * s(t - \tau_m(\theta)) + n_m(t) \tag{2}$$

where $h_m(t)$ is the impulse response of the mth sensor, $*$ denotes the convolution and $n_m(t)$ is additive noise. $h_m(t)$ is assumed to be equal to $\delta(t)$ due to the assumption about identical sensors. Since the signal is considered narrowband, the amplitude $u(t)$ and the phase $\phi(t)$ can be assumed to vary slowly relative to the propagation time along the array, which gives

$$u(t - \tau_m) \approx u(t) \tag{3}$$

$$\phi(t - \tau_m) \approx \phi(t). \tag{4}$$

2.3.2 Assumptions

The list below describes some of the assumptions that have been used in the bearing estimation:

- The received signals are assumed to be composed of harmonics, i.e. narrowband signals.
- The signal source and the sensors in the array are assumed to be in the same plane. This means that the angle between the y-axis and the wave projektion in the x-y plane is considered to be $0°$.
- The signals from the sources and the ambient noise are assumed to be independent and, hence, uncorrelated.
- The source is in the far-field, and the waves arriving at the array is assumed to be planar.
- The wave propagating media is assumed to be homogeneous and non-dispersive.
- The ambient noise is considered to be isotropic, i.e. spatially white noise with equal power from every direction.

- The sensors are assumed to be identical and omni-directional, and equally spaced over the entire array. The distance between two adjacent sensors is $d < \frac{\lambda}{2}$ to avoid aliasing according to the spatial sampling theorem.

2.3.3 Physical Limitations

Due to the array, some physical limitations have to be considered:

- Geometric constraints. The bearing estimate has a larger error when the source is close or passes the End Fire of the linear array than when the source is located at Broad Side of the linear array. This depends on that the width of the beam is increased when the source moves away from the array Broad Side, and the properties of the arcsine function.
- Ambiguity. Because the array aperture is only used in the half-plane (180°) it is impossible to avoid North-South ambiguity. This means that a source can be located at both the north and south side of the ULA, and still yield the same bearing estimate. The North-South ambiguity is shown in Figure 1.

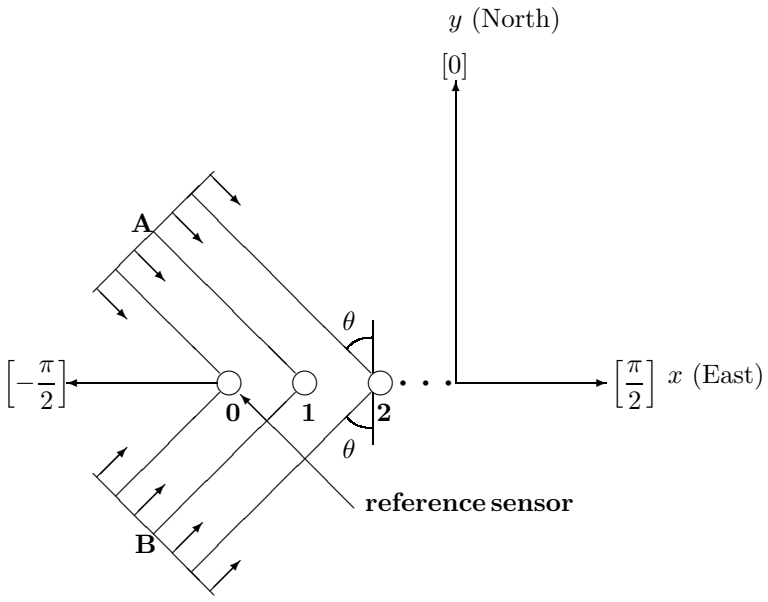

Figure 1: *One ULA cannot unambiguously determine if there is wavefront* **A** *or* **B** *that gives bearing* θ *(North-South Ambiguity).*

3 Bearing Estimation

To detect and determine the bearing of a far-field radiating source different types of antenna arrays can be used, for example a linear array (Uniform Linear Array, ULA) or a circular array. Only the properties of the linear array will be addressed in this thesis.

When using a passive sonar system with a ULA, the location of the source can not fully be established without using several arrays that are separated from each other in space. By estimating a bearing for each array and then combining the bearing estimates, the location can be determined by triangulation or by using hyperbolas.

Figure 2 shows a plane wave front incoming towards a Uniform Linear Array (ULA) from bearing θ. As can be seen in Figure 2, the wave front will hit the M sensors in the linear array, with a time delay τ_m between the sensors, dependent on the bearing θ. Sensor 0 will further on be referred to as the reference sensor in the linear array.

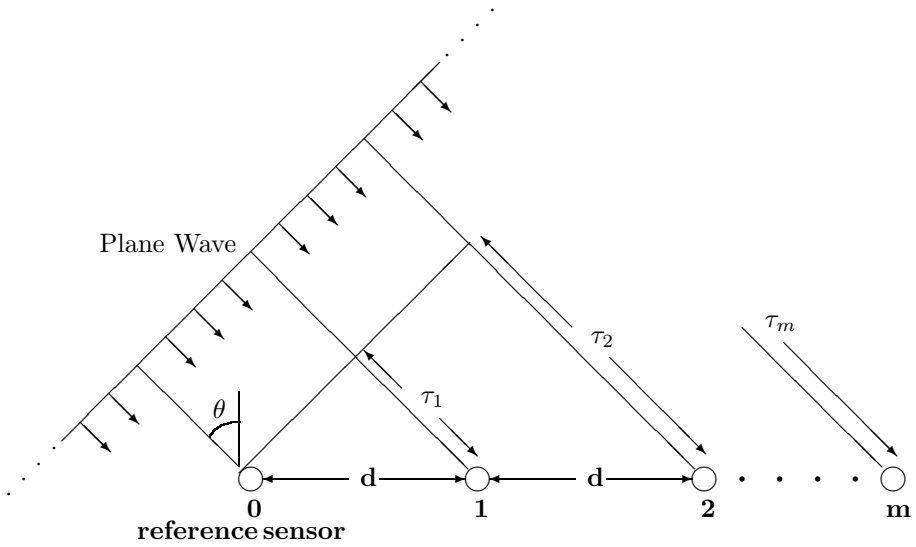

Figure 2: *How a plane wave front approaching a linear acoustic sensor array. Due to the bearing θ, there will be a time delay τ_m between the wave received by sensor 0 and sensor m ($m = 0, ..., M-1$). Sensor 0 is the reference sensor in the linear array.*

The distance d (see Figure 2) between two adjacent sensors, must be chosen from the minimum wavelength λ that is expected to be received at the array. This is to avoid aliasing that will affect the bearing estimation in a negative way. Eq. 5 shows how a proper value of d can be chosen [16]

$$d \leq \frac{\lambda}{2} \tag{5}$$

The resolution of a linear array is dependent on the physical properties of the array (array length, distance between sensors etc.). It is a measure for the ability to resolve two closely spaced sources. Problems occur when the two sources are so close in bearing that their main lobes melt together to one and they can not be distinguished as two different sources. This is illustrated in Figure 3, where the two sources, **A** and **B**, are treated as one source **C** if they

are too closely spaced (upper figure) and are recognized as two separate sources if the bearing separation between them is large enough (lower figure). As seen in Figure 3 the separation of

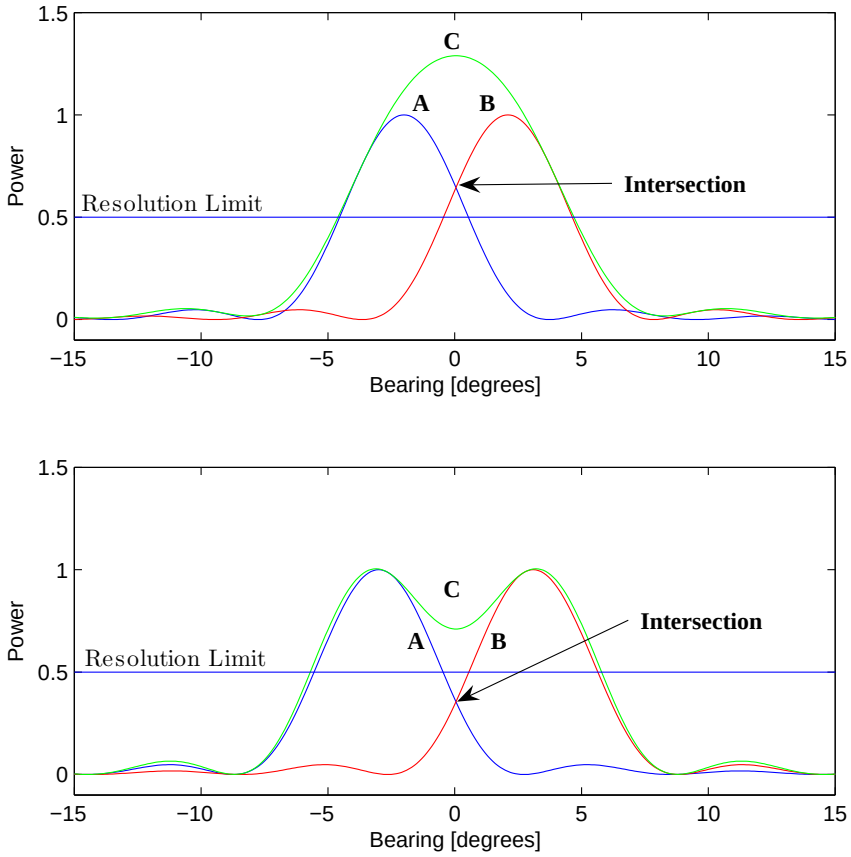

Figure 3: *The upper figure describes the situation when the two sources (***A** *and* **B***) are so closely spaced that they cannot be separated. They are assumed to be only one source (***C***). In the lower figure the two sources (***A** *and* **B***) are enough separated from each other to be identified as two different sources.*

the two sources is dependent on whether the intersection between the two main lobes is above or below the resolution limit. The resolution limit is set to half (0.5) the maximum power for the weakest source (3 dB below max power in decibel scale). Two curves that have an intersection above this limit automatically melt together, and it is impossible to identify them.

By using the information received about the time delays τ_m at every sensor in the array, the direction of arrival (DOA) can be estimated. The estimate can be determined with several different methods, with different performance. The methods that are described in this thesis are Conventional Beamforming (Section 3.2), MV (Section 3.3) and MUSIC (Section 3.4).

In all three methods, the SCM is of great importance, in order to obtain reliable bearing estimates. To obtain a small bearing estimate error the SCM has to be well estimated. The estimation of the SCM is discussed in Section 3.1.

3.1 Spatial Covariance Matrix

The Spatial Covariance Matrix (SCM) plays an important role in the bearing estimation of the source. The SCM carries the information about the intersensor correlation and the phase difference that is used in the estimation of the bearing. To obtain an accurate estimate, the matrix has to be well formed. This is dependent on how many snapshots that are used in the estimation of the SCM. More snapshots gives a more accurate estimation (if the data are stationary) but is more computer time consuming. The issue is to find a number of snapshots that satisfy the stationarity demands and gives a sufficient accuracy with a minimal computer time consumption. Figure 4 describes how the snapshot vectors are determined.

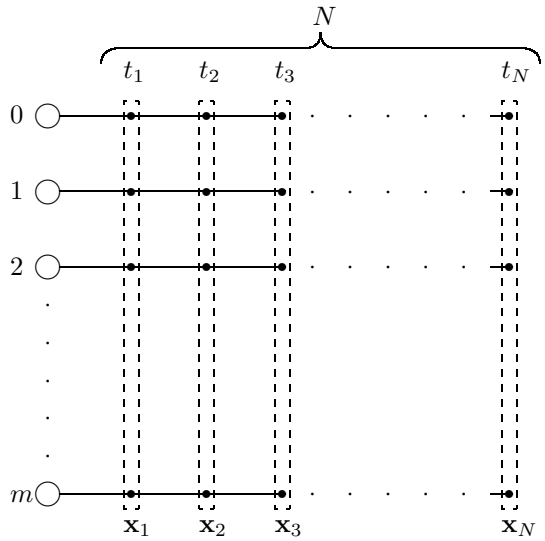

Figure 4: *Description of how the snapshot vectors* $\mathbf{x}_i$ *are defined from the incoming data stream. By taking one sample from each channel at a certain time* t_i *(snapshots) a snapshot vector* $\mathbf{x}_i$ *can be formed. If the incoming data at every channel, has a block length* N*,* N *snapshot vectors* $\mathbf{x}_i$ *can be formed.*

As seen in Figure 4 the number of snapshot vectors $\mathbf{x}_i$ are determined by the amount of incoming data, received at every sensor (the block length N). Each snapshot vector is defined by taking one sample from each sensor at a certain time t_i.

Figure 5 describes the relationship between the condition number of the SCM and the number of snapshots, N, used. The Matlab function *cond* is used to compute the condition number of the SCM. A high value represents an ill conditioned SCM and a low value a well conditioned SCM.

The condition number of a matrix is traditionally a measure of the stability to numerical operations. It is computed from the realtionship between the maximum and the minimum eigenvalue of the matrix [1], [6], [8]. One purpose with the thesis is to study if the condition number of the SCM can be used as a feature to determine the amount of data that shall be used to estimate the DOA. The DOA of the source is related to the eigenvectors of the SCM not the eigenvalues. Therefore, the connection between the condition number and the DOA estimate is weak, but it can still be used as a measure of when the SCM is well estimated (i.e.

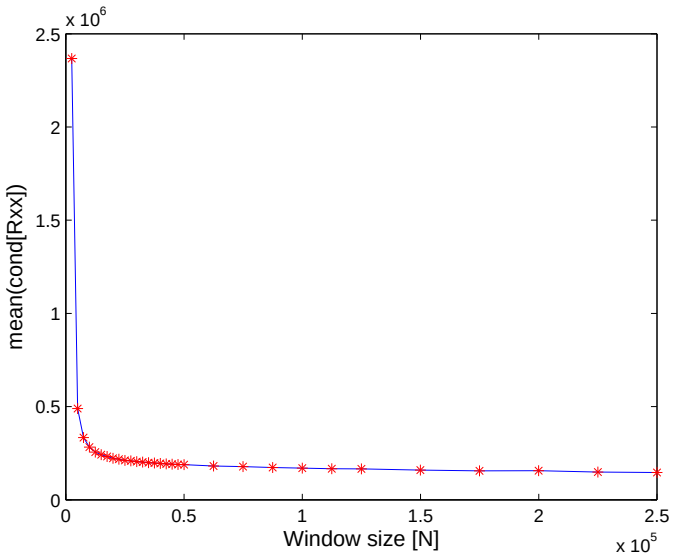

Figure 5: *The condition number of* $\mathbf{R}_{xx}$ *decreases when the number of snapshots* N *increases. A smaller condition number represents a more well conditioned SCM which means that the SCM becomes better conditioned when the number of snapshots* N *increases. The values shown are the mean value for the condition number during the entire recording for each length on the estimation window. The values are estimated from Track 1, see Chapter 4.*

when the estimator has reached its asymptotic region, see Figure 5) [5]. The condition number of the SCM is dependent on the Signal-to-Noise Ratio (SNR), a higher SNR will result in a higher condition number of the SCM. However, a higher SNR will result in an improved DOA estimate. The interesting part is to see the relative change of the condition number, not the absolute value. The trend shown in Figure 5 will still be the same for different SNR levels, the axis is only rescaled. The length of the estimation window is chosen from the point where the relative change of the condition number is small (i.e. choosing a longer estimation window will not result in significantly better condition number).

Per definition the SCM is given by the expected value of the squared snapshot vector as

$$\mathbf{R}_{xx} = E\{\mathbf{x}\,\mathbf{x}^H\} = E\begin{Bmatrix} x_1\,x_1^* & \dots & x_1\,x_M^* \\ \vdots & \ddots & \vdots \\ x_M\,x_1^* & \dots & x_M\,x_M^* \end{Bmatrix} = \begin{Bmatrix} E\{x_1x_1^*\} & \dots & E\{x_1x_M^*\} \\ \vdots & \ddots & \vdots \\ E\{x_Mx_1^*\} & \dots & E\{x_Mx_M^*\} \end{Bmatrix} \tag{6}$$

where $\mathbf{x} = [x_1, x_2, ..., x_M]$ and M is the number of sensors in the array. In real cases there is a limited number of snapshot vectors $\mathbf{x}_i$ available and the SCM must therefore be estimated correspondingly. This can be done in many different ways, depending on the existing demands on accuracy and stability. The method chosen in this thesis to estimate the SCM, is

$$\widehat{\mathbf{R}}_{xx} = \frac{1}{N}\sum_{i=1}^{N}\mathbf{x}_i\mathbf{x}_i^H \tag{7}$$

where i is the snapshot number and N is the total number of snapshots (window size). As can be seen in Eq. 7, $\widehat{\mathbf{R}}_{xx}$ is an estimate using N snapshot vectors $\mathbf{x}_i$. This means that the actual

estimated SCM is an average value of N calculated instantaneous SCMs, which will, due to the averaging, have a lower variance than a SCM without averaging.

When tracking a target during a certain time, several SCMs have to be estimated, representing different motion of the bearings as the source moves. A problem can occur when the estimate of the SCM is poor, e.g. due to low SNR or some disturbances (e.g. multipath). If the source is moving slowly between every measurement (i.e. the incoming signal has relatively long stationarity time), the information from the previous estimated SCM can be used, when estimating the new SCM. In this way a better conditioned estimate of the SCM can be achieved, and therefore the bearing estimate is improved. This is called recursive updating and is done as [4],[17]

$$\widehat{\mathbf{R}}^{(n)} = \alpha\widehat{\mathbf{R}}_{xx}^{(n)} + (1-\alpha)\widehat{\mathbf{R}}^{(n-1)} \tag{8}$$

where n is the n:th estimation window with the initial value $\widehat{\mathbf{R}}^{(0)} = \mathbf{0}$. $\widehat{\mathbf{R}}^{(n)}$ is the n:th estimated SCM that will be used in the bearing estimation.

By choosing different values for the constant α ($0 < \alpha < 1$), it can be decided how much information about the previous SCM is used, in the estimation of the new SCM. There is no single value for α that is optimal for every occasion. There are several methods that can be used to choose a proper value of α to fit under some criteria. Some methods to choose α are listed below:

1. α is a static value during the entire measurement.
2. The value of α is chosen from the SNR, which will be varying under the entire measurement. When the SNR is low, a lower value of α is chosen and so on. In this way bad estimates dependent on bad current SNR can be avoided, and instead use more information from the previous SCM estimate.
3. Use several different α values, and estimate the SCM for each one. Choose the SCM with the best condition number at every time interval.
4. The value of α is chosen by the correlation between the signal received at the reference sensor (see Figure 2) and the signal received at one optional sensor. By using the correlation between the two sensors an indication of the SNR is achieved as well as a possible bearing.
5. Similar to the previous method is to choose α from the correlation between two consecutive estimation windows.

3.2 Conventional Beamforming

Conventional Beamforming (CB) is the most commonly used method in estimating the direction of arrival. The aim of this method is to mathematically simulate a steering of the arrays main beam in a desired direction. Every direction is built up by different time delays τ_m applied on the sensor output signals x_m. In this way it is possible to simulate the array looking in the directions of interest and by that finding the bearing to the source. This is defined as, [10]

$$y(t) = \sum_{m=0}^{M-1} w_m x_m(t-\tau_m) \tag{9}$$

where M is the number of sensors used in the array, $m = 0, \ldots, M-1$, x_m represents the signals from the M sensors, w_m is weights and τ_m represents different time delays at the sensors that

is used to simulate the direction of interest. Every direction has a set of different time delays starting from a reference sensor (see Figure 2). The weights w_m can be chosen in many ways, for example to represent a Gaussian or Kaiser window to suppress the side lobes etc, but will in this thesis be set to unity (rectangular window) for simplicity.

To find an estimate of the bearing to a source, the power $\mathbf{P}$ of the beam can be estimated in every direction that the array is steered in. In this way, the power $\mathbf{P}$ becomes a function of the direction. The direction that gives the maximum value for $\mathbf{P}$ is assumed to be the direction of the source. This is illustrated in Figure 6, where the power $\mathbf{P}$ is plotted as a function of the bearing.

To get deeper understanding of the beamforming method, it can be an advantage to transform it to the frequency domain as

$$Y(f) = \sum_{m=0}^{M-1} w_m e^{-j2\pi f \tau_m} X_m(f). \tag{10}$$

The expression for the Fourier transform of the beam, can be rewritten as a dot product of two vectors, for every frequency f as

$$Y(f) = \mathbf{S}^H \mathbf{X} \tag{11}$$

where $\mathbf{S}$ represents the steering vector as a function of f (f is chosen according to the frequency of the signal of interest). $\mathbf{S}$ is expressed as

$$S_m(f) = w_m e^{+j2\pi f \tau_m} \tag{12}$$

where m corresponds to sensor m and so on. The time delay τ_m between the sensor signals can be formed as an expression of the angle θ (DOA)

$$\tau_k = \frac{kd}{c}\sin(\theta) \quad k = 1, \ldots, M-1 \tag{13}$$

where c is the propagation speed of sound in water, d is the distance between two adjacent sensors, and k is the k:th sensor from the reference sensor (see Figure 2). By using Eq. 13 in Eq. 12 the steering vector is given as

$$S_m(\theta) = w_m e^{+j2\pi f \frac{kd}{c}\sin(\theta)}. \tag{14}$$

The total power $\mathbf{P}$ of the steered signal $Y(f)$ can be expressed as an expectation value for each direction θ as

$$\mathbf{P}(\theta) = E\{|Y(f)|^2\}. \tag{15}$$

If $Y(f)$ in Eq. 15 is substituted by the expression in Eq. 11 this gives

$$\mathbf{P}(\theta) = E\{|\mathbf{S}^H\mathbf{X}|^2\} = E\{\mathbf{S}^H\mathbf{X}\mathbf{X}^H\mathbf{S}\}. \tag{16}$$

The received signal is assumed to be a narrowband signal with frequency f_0. This leads to that the steering vector $\mathbf{S}$ in Eq. 16 can be considered as a constant, fixed at f_0, only dependent on the present direction θ. Eq. 16 can now be simplified to

$$\mathbf{P}_{cb}(\theta) = \mathbf{S}^H(\theta)\mathbf{R}_{xx}\mathbf{S}(\theta) \tag{17}$$

where $\mathbf{R}_{xx}$ is the Spatial Covariance Matrix (See Section 3.1)

$$\mathbf{R}_{xx} = E\{\mathbf{X}\mathbf{X}^H\}. \tag{18}$$

Eq. 17 shows the true power $\mathbf{P}(\theta)$ of the signal in every direction θ and is the expression that is used for CB. This expression is valid for one or several sources when they have the same frequency. But if there is several sources with different frequencies present, a steering vector $\mathbf{S}(\theta)$ has to be formed for each frequency. Since the steering vector in Eq. 14 only depends on the direction θ that the array is steered at, an error in other parameters will create a bias to the estimate. The propagation speed c is presumably the largest factor to the bias but also an error in the distance d and the frequency f will create a bias.

CB is a rather uncomplicated and robust method to implement, but has a major drawback in its low resolution ability. The resolution is limited by the width of the beam, which is set by the physical constraints of the array (array length and distance between sensors). The bearing separation θ that is required to identify two closely spaced sources with a linear array with uniform receiving along the array, can be described by [18]

$$\theta_{CB} = \frac{C\lambda}{L} \tag{19}$$

where λ is the wavelength for the signal, L is the length of the array ($L = (M-1)d$), d is the distance between two adjacent sensors and C is a constant [18]. C is dependent on the weights w_n in equation Eq. 14 and therefore the resolution can be changed by using other weights (e.g. Gaussian or Hanning window etc.). With present weights the constant C is 50.5° The required bearing separation can also be explained by the Rayleigh criteria [14]. Figure 6 illustrates a situation when there are two sources present and CB is used.

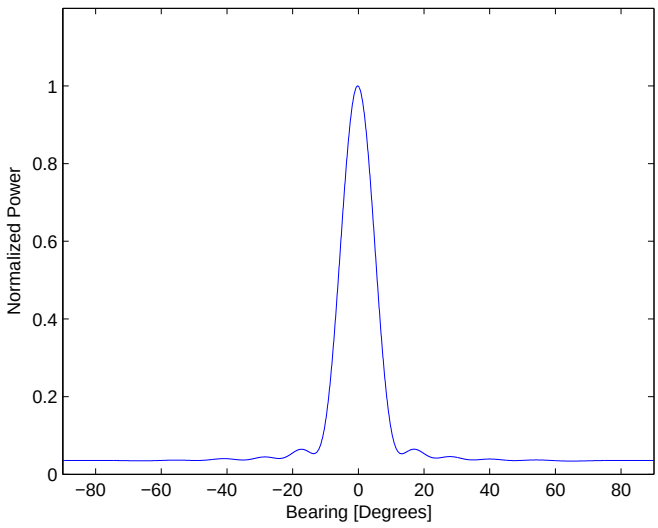

Figure 6: *The Power-Bearing spectra, estimated with CB. There are two sources with Gaussian random noise present, and they are located at bearings -3 and 3 degrees. The sources are uncorrelated with each other and the noise. The number of sensors used in the array is 20. As seen, the CB method cannot resolve the two sources under present conditions.*

As seen in the figure the two sources cannot be resolved, dependent on the limited resolution that is achieved with CB. The resolution can be increased by increasing the length of the array which will give a more narrow beam. In this case CB would be able to resolve the two sources.

Some of the advantages and disadvantages with CB are listed below [2], [9], [10], [16]:

Advantages:

- Analytical expressions for bearing performance.
- Easy to understand and implement, both in the time- and frequency domain.
- More robust against correlated signals than the MV and MUSIC method.
- Robust against errors in the assumed signal model, such as the sensors location in the array, the noise distribution and the shape of the wave front.
- Gives an estimate of the power as a function of the bearing (see Eq. 17).
- Relatively stable for broadband signals, even if it is designed for narrowband signals.

Disadvantages:

- Low resolution performance. The physical constraints of the array set the limit.
- High side lobes, which can be suppressed by different weighting but to the cost of increased width of the main lobe and therefore lower resolution.
- Significant bias in the estimation of the bearing can occur when a very broadband signal is present.
- Sensitive to a low SNR and gives a high estimated variance when few snapshots are used.

To improve the resolution (to be able to resolve too closely spaced sources) with CB the array length has to be increased. If the array length is limited there is a need to find other methods with better resolution properties that can resolve the sources with the available array length. Two of these methods are described in the two next chapters, one nonparametric and one parametric method.

3.3 Minimum Variance Method

As have been shown in the previous section CB suffers from the inability to resolve two closely spaced sources within the beam width. One approach to solve this is to use the Minimum Variance method (MV), where the idea can be described in two steps [16]:

1. The signal with the desired DOA passes undistorted.
2. Every other signal with different DOA will be attenuated as much as possible.

This is achieved by minimizing the output power $\mathbf{P}(\theta)$ in every direction θ under the condition that a pure sinus signal can pass undistorted. This is equal to minimizing the variance in every direction, whence the name Minimum Variance Method. The minimization problem can be written as

$$\mathbf{P}(\theta) = \mathbf{A}^H \mathbf{R}_{xx} \mathbf{A} \tag{20}$$

$$\min_A \mathbf{A}^H \mathbf{R}_{xx} \mathbf{A} \quad \text{subject to} \quad \mathbf{A}^H \mathbf{Z} = 1 \tag{21}$$

where $\mathbf{A}$ is the steering vector with weights w_m and $\mathbf{Z}$ is a constraint vector. The solution to this optimization problem is [2], [9], [10]

$$\mathbf{A} = \frac{\mathbf{R}_{xx}^{-1}\mathbf{Z}}{\mathbf{Z}^H\mathbf{R}_{xx}^{-1}\mathbf{Z}}. \tag{22}$$

By using the optimized expression for $\mathbf{A}$, where the constraint vector $\mathbf{Z}$ is chosen to be equal to the steering vector $\mathbf{S}(\theta)$ in Eq. 12, in Eq. 20 the following expression for the power $\mathbf{P}(\theta)$ is obtained

$$\mathbf{P}_{MV}(\theta) = \frac{1}{\mathbf{S}^H(\theta)\mathbf{R}_{xx}^{-1}\mathbf{S}(\theta)}. \tag{23}$$

This is the expression that is used for DOA estimation with MV. The directions with the maximum power are considered as estimations of the DOAs. Figure 7 shows the bearing estimation made with MV, with the same signal sources and under the same conditions as in Figure 6 with CB. As can be seen in the figure the two sources are clearly separated with MV, which they were not with CB.

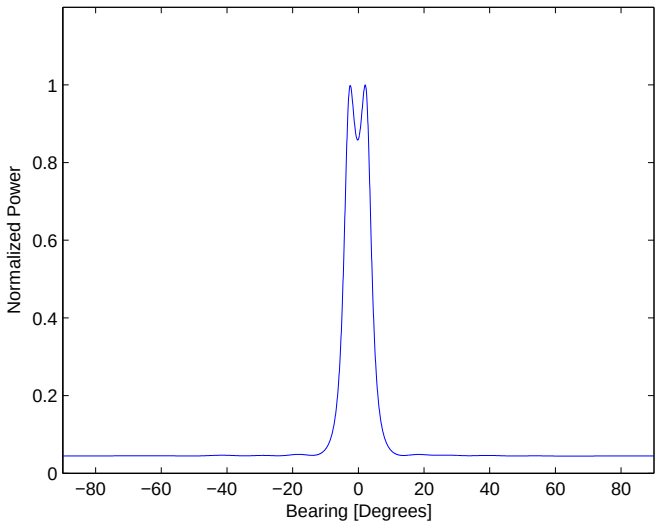

Figure 7: *The Power-Bearing spectra, estimated with MV under the same conditions as in Figure 6. As seen, the sources can be resolved with this method.*

To be sure that the inverse of the SCM exists or is non-singular, enough snapshots have to be used in the estimation of the matrix. The resolution is also improved by using more snapshots, i.e. longer estimation window.

It has been empirically proved that MV possesses a superior performance, in the DOA estimation, compared with CB. This is true when the desired signal is uncorrelated with the interference. When correlation between signals occurs, e.g. in multipath propagation, MV will give a worse result than the more robust CB method. The reason for this behaviour is that the minimization will result in a cancellation of the desired signal, where the amount of cancellation depends on the correlation. An advantage with MV is that the variance is lower, i.e. lower side lobes than CB.

The bearing separation θ_{MV} with MV can be described with the approximate relation between θ_{MV} and the wavelength λ, the array length L, the number of sensors M and the Signal-to-Noise Ratio (SNR), $\frac{P_s}{P_n}$, [10]

$$\theta_{MV} \approx \left(\frac{MP_s}{P_n}\right)^{1/4} \frac{\lambda}{L} \tag{24}$$

where θ_{MV} is given in radians. Below some advantages and disadvantages with MV are listed [2], [9], [10], [16]:

Advantages:

- Superior resolution compared to CB when the number of sources is small relative the number of sensors in the array.
- Gives an estimate of the power that is proportional to the true power.
- Gives the largest antenna gain of all beamforming methods.
- Quite stable for broadband signals, although it is designed for narrowband signals.

Disadvantages:

- Sensitive to a low SNR and to a small number of snapshots.
- Longer computational time than CB.
- Relatively large bias can occur for very broadband signals.
- More sensitive to correlation between the signal and any interference than CB.

3.4 Subspace Methods

The two methods described in Section 3.2 and Section 3.3 are both so called non-parametric methods. One advantage with those methods is that they do not need the information about the statistical properties of the data, like parametric methods do, to create reliable DOA estimates. A parametric method on the other hand gives a better performance than a non-parametric method when the statistical information is available [16].

This section will describe two very similar parametric methods: the Eigenvector method (EV) and the MUSIC (Multiple Signal Classification) method. These use information about the eigenvalues and the eigenvectors of the spatial covariance matrix $\mathbf{R}_{xx}$ to estimate the DOA.

The approach in both methods is to find a constraint vector $\mathbf{Z}$ (see Section 3.3, Eq. 21) that maximizes the resolution. $\mathbf{Z}$ can for example be chosen as

$$\mathbf{Z} = \mathbf{C}\mathbf{S}(\theta) \tag{25}$$

where $\mathbf{S}(\theta)$ is the steering vector and $\mathbf{C}$ is the unknown matrix. By using Eq. 25 in Eq. 20 this yields

$$\mathbf{P}(\theta) = \frac{1}{\mathbf{S}^H(\theta)\mathbf{C}^H\mathbf{R}_{xx}^{-1}\mathbf{C}\mathbf{S}(\theta)}. \tag{26}$$

If it is possible to create a matrix $\mathbf{C}$ so that $\mathbf{C}\mathbf{S}(\theta) = 0$, when $\mathbf{S}(\theta)$ points in a direction of a source, this will end up in an infinite energy response in that direction. This should in theory

give a perfect indication of the bearing. In practice $\mathbf{CS}(\theta)$ is never equal to zero, but it will be very small. The difficulty is to find a value of $\mathbf{C}$ that fulfils this [10].

Eigenvector method and MUSIC

The issue with subspace methods is to separate the total space into a signal subspace (where the signal is present) and a noise subspace (where the ambient noise is present). The signals that are received from the M sensor outputs can be described as

$$x_m(t) = s_m(t) + n_m(t) \quad m = 1, \ldots, M \tag{27}$$

where s_m is the signal received at sensor m and n_m is the noise that is present at sensor m. Through this equation the SCM (see Section 3.1) can be formed and separated into a signal part and a noise part as

$$\mathbf{R}_{xx} = \mathbf{R}_{ss} + \mathbf{R}_{nn} \tag{28}$$

where $\mathbf{R}_{ss}$ represents the spatial covariance matrix for the signal and $\mathbf{R}_{nn}$ for the noise. To achieve this decomposition the eigenvalues and eigenvectors of $\mathbf{R}_{xx}$ are estimated according to

$$\mathbf{R}_{xx}\mathbf{V}_i = e_i\mathbf{V}_i \tag{29}$$

where e_i is the eigenvalue associated with the eigenvector $\mathbf{V}_i$. From the decomposition of $\mathbf{R}_{xx}$ M eigenvalues is obtained. The p largest of those eigenvalues are assumed to correspond to signals, and the associated eigenvectors span the signal subspace where the signal vectors can be found. The number of sources is not necessary the same as p (p is the same as the number of sources if the noise is white guassian noise), but the signals are certainly in the subspace that is spanned by the eigenvectors. The $M - p$ smallest eigenvalues are assumed to correspond to noise and the associated eigenvectors span the noise subspace. The eigenvectors that span the signal subspace are all orthogonal to the eigenvectors that span the noise subspace [10].

Because it is not certain that the p largest eigenvalues correspond to p signal sources, the $M-p$ eigenvalues that correspond to noise is used for the estimation of the bearing/bearings. The advantage of using the noise subspace to search for the source is that when the beam is steered in the direction of the source, the value of $\mathbf{CS}(\theta)$ will be very small. The result of this is a sharp high peak, which is substantially higher compared to the directions of only noise.

The unknown matrix $\mathbf{C}$ can be defined as [10]

$$\mathbf{C} = \sum_{i=1}^{M-p} \mathbf{V}_i\mathbf{V}_i^H. \tag{30}$$

where $\mathbf{V}_i$ is the eigenvectors that span the noise subspace. The SCM, expressed in terms of the eigenvectors $\mathbf{V}_i$, can be defined as

$$\mathbf{R}_{xx} = \sum_{i=1}^{M} e_i\mathbf{V}_i\mathbf{V}_i^H \tag{31}$$

with its inverse

$$\mathbf{R}_{xx}^{-1} = \sum_{i=1}^{M} \frac{1}{e_i}\mathbf{V}_i\mathbf{V}_i^H. \tag{32}$$

If the Eq. 30, 31 and 32 are used in Eq. 26, this will give

$$\mathbf{P}_{ev}(\theta) = \frac{1}{\sum_{i=1}^{M-p} \frac{1}{e_i} \left|\mathbf{S}^H(\theta)\mathbf{V}_i\right|^2}. \tag{33}$$

This equation in its direct form is called the Eigenvector Method (EV) and the very popular MUSIC algorithm is obtained by setting all noise eigenvalues e_i to unity

$$\mathbf{P}_{music}(\theta) = \frac{1}{\sum_{i=1}^{M-p} \left|\mathbf{S}^H(\theta)\mathbf{V}_i\right|^2} \tag{34}$$

Both these methods have superior bearing resolution compared with the previously described methods, under advantegeous conditions. When there are errors in the assumed model, such as erroneous estimates of p, the bearing resolution will be seriously decreased. p is the estimated number of the eigenvectors $\mathbf{V}_i$ that span the signal subspace. The effects of an improper choice of p is,

- If p is chosen to 0 (poor SNR etc.) MUSIC will show a flat spectrum with no peaks. EV will show exactly the same result as MV.
- If p is chosen smaller than the true number of sources, the resolution will not be superior to MV. EV will have the same bearing resolution properties as MV, but the resolution with MUSIC will be decreased. MUSIC will always show the same number of peaks as the number of p. On the other hand, the peaks that are shown are almost at correct bearings.
- If p is chosen larger than the true number of sources, the bearing resolution is minimally decreased. EV will give the same number of peaks as with a correct estimate of p and MUSIC will give some extra spurious peaks, but will show the correct ones as well.

Figure 8 shows the bearing resolution with the MUSIC method with the same signals and conditions as with CB and MV in Figure 6 and 7. As can be seen in the figure MUSIC gives two distinct peaks that clearly show that there are two sources present. The resolution is much better than with MV and superior to CB. The variance is also smaller.

The improved resolution when using subspace methods, like EV and MUSIC, is because they create a synthetic value for the number of sensors in the array, and therefore a synthetic array length. The synthetic value $\widetilde{M}$ (number of synthetic sensors) is in most cases larger than the true number of sensors M, existing in the array. The synthetic value $\widetilde{M}$ is a quantity of how the resolution is improved with EV and MUSIC, and is described in [10] as

$$\widetilde{M} = \frac{1}{\frac{P_n}{P_s}\frac{\gamma^2}{M^2} + \frac{1}{N}} \tag{35}$$

where γ is an estimate for the spreading of the noise eigenvalues e_i and N is the used window size (number of snapshots). In general, γ will decrease with an increasing value of N, and tends towards zero (noise covariance matrix is equal to the identity matrix). The first denominator term in Eq. 35 determines the magnitude of the energy peak and the second denominator term describes the relation between the size of the energy peak and N. Because of the relation between γ and N one of these terms will dominate. The synthetic array length $\widetilde{L}$ can be described as

$$\widetilde{L} = (\widetilde{M} - 1)d. \tag{36}$$

If the result in Eq. 35 and Eq. 36 is used as the value for M and L in Eq. 24, this gives the expression [10]

$$\theta_{MUSIC} \approx \left(\frac{\frac{P_s}{P_n}}{\frac{P_n\gamma^2}{P_sM^2} + \frac{1}{N}}\right)^{1/4} \frac{\lambda}{\widetilde{L}} \tag{37}$$

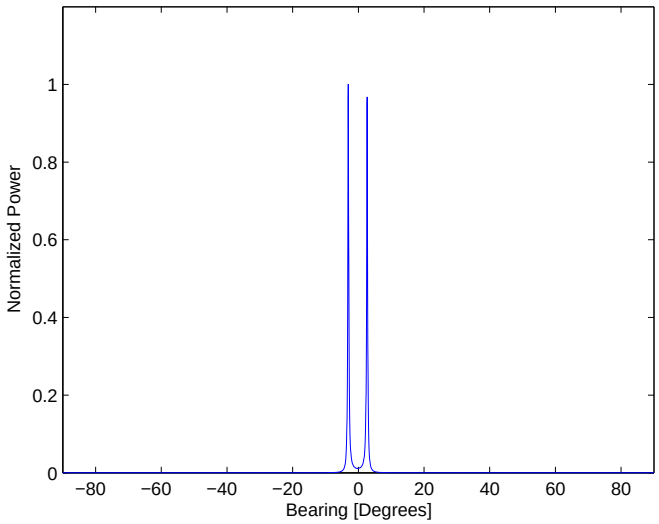

Figure 8: *The Power-Bearing spectra, estimated with the MUSIC method under the same conditions as in figure 6 and 7. MUSIC gives two distinct peaks at the bearings of the two sources. The magnitude of the peaks do not give an indication about the power of the sources only that the sources are located in these directions. The value of p is chosen to* 2.

where θ_{MUSIC} is given in radians. Below some advantages and disadvantages with EV and MUSIC are listed [2], [9], [10].

Advantages:

- Can resolve the sources with a very high resolution, even if they are closely spaced and/or weak.

Disadvantages:

- Will not give a true power spectrum.
- Poor broadband properties.
- CPU time consuming.
- The array gain is decreased as a result of better bearing resolution.
- Sensitive to errors in the assumed model, e.g. wrong number of sources, correlation between signals because of multipath propagation etc.

3.5 Number of Sources Estimation

As mentioned in Section 3.4 the benefits obtained with subspace methods are in theory substantially dependent on the selected value of p. In real applications the value of p is not always known and must therefore often be estimated in some manner to obtain the benefits that the subspace methods yields.

The method used in this thesis uses the gradient of the eigenvalues e_i to estimate the value of p. The idea is to find where the gradient of the eigenvalues e_i has its maximum value. This maximum point is assumed to correspond to the optimal choice for p to obtain best bearing performance. The principle of the method is illustrated in Figure 9. As can be seen in the figure the optimal value for p is 2 in the illustrated case.

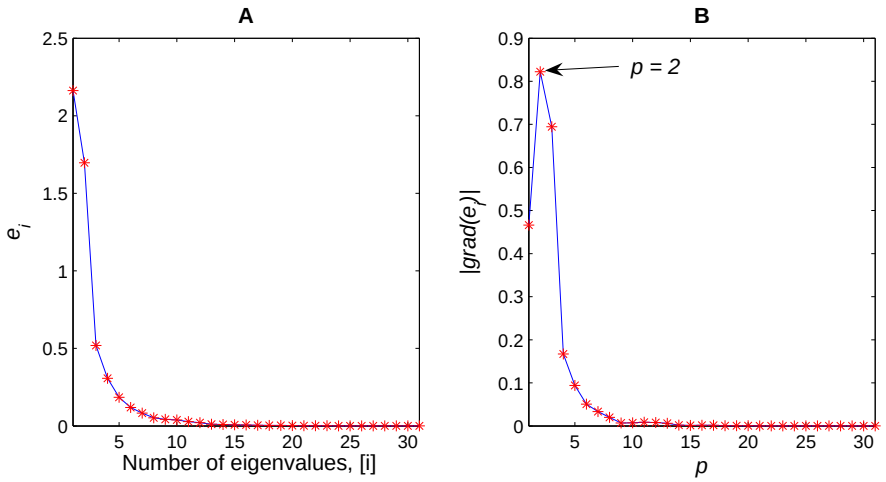

Figure 9: *Part* ***A*** *shows the eigenvalue* e_i *for a possible situation and part* ***B*** *shows the corresponding gradients. As can be seen the optimal value on* p *is in this case* 2.

Another method that can be used to estimate the number of sources is known as the MDL criterion (Minimum Description Length). The MDL criterion is known to be a consistent estimator and robust against deviations in the Gaussian assumption model. This method will not be used or evaluated in this thesis, but is further described in previous work by [4], [17]

4 Real Data

To evaluate the performance of the described bearing estimating algorithms they are evaluated with real measured data. The data were recorded at a sea trial that was conducted in the southern part of the Stockholm archipelago between August 12-26, 2004. The average depth at the trial site was 40 m which is a typical depth for the shallow water in this part of the Baltic Sea. The array that was used is a Uniform Linear Array, horizontally placed on the sea bed, with 1.5 m spacing between adjacent acoustic sensors. This sensor spacing allows the array to receive frequencies up to 500 Hz, without aliasing effects according to the spatial sampling theorem [16]. The acoustic sensors are omni-directional, calibrated for the frequency range $200 - 2000$ Hz. The array consists of 31 acoustic sensors which gives a total array length of 45 m. Received data from the source were sampled with a sampling frequency of 25 kHz.

The bearings are restricted to one half-plane (180°) to avoid the ambiguity described in Chapter 3. The chosen interval is $[-90°; 90°]$, where 0° represents a bearing right in front of the array (Broad Side) and $\pm 90°$ a bearing at the periphery of the array (End Fire).

In the evaluated measurements two different vessels occur, the experiment vessel HMS Ägir and FOI's vessel Decibella. Each vessel creates a signature that can be used for the bearing estimation. The signature is dependent on the velocity for the vessel.

Track 1

Track 1 is a recording of the vessel Ägir when it is equipped with the acoustic signal source RAMSE that transmits a 200 Hz signal. RAMSE is towed behind Ägir at an average depth of 7 m according to Figure 10. Ägir moves with an average velocity of 3.4 *knots*.

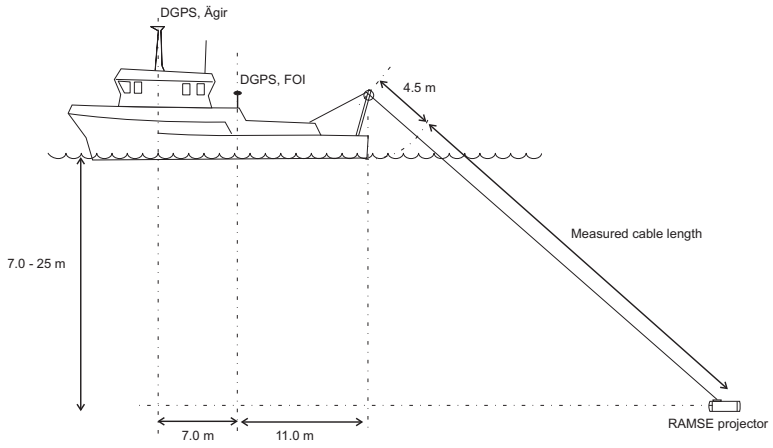

Figure 10: *The figure shows the vessel, HMS Ägir, with the towed signal source. The towed signal source transmits a signal with a frequency of 200 Hz.*

Ägir moves according to the DGPS track in Figure 11, where the location of the used array aperture is marked with a black line.

The DGPS track can be used to transform the positions of the vessel to bearings relative the linear array every second (e.g. sampling frequency of 1 Hz). These bearings are used to verify the performance for the bearing estimation algorithms. The obtained bearing curve for the DGPS track is shown in Figure 12.

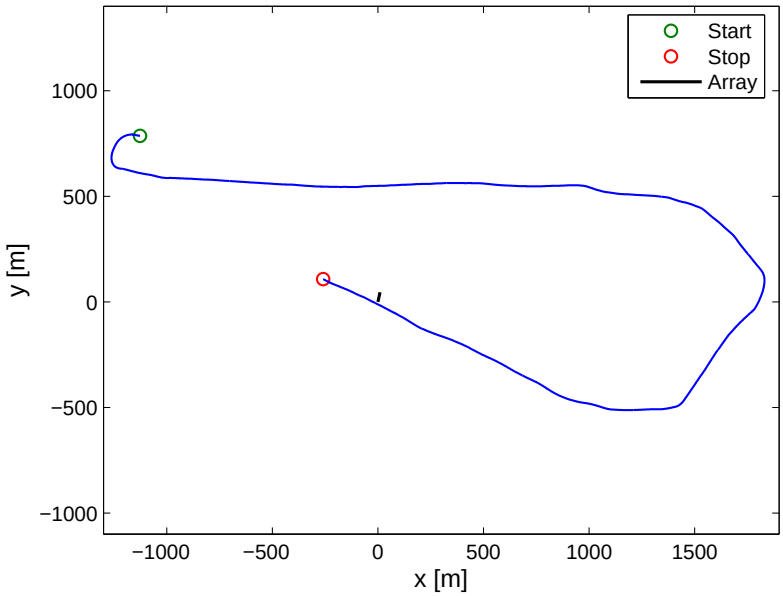

Figure 11: *The figure shows the DGPS track for Ägir in recording Track 1. The black thick line represents the ULA and the green and red circles represent the start and end of the DGPS signal.*

The sharp peaks in Figure 12 that appears at about 1000 s and 3350 s are the times where the vessel passes the arrays End Fire. Because of the ambiguity, the bearing curve turns back towards 0°.

The spectrogram of the recorded signal for *Track 1* when a 1 s estimation window is used is displayed in Figure 13. Apart from the 200 Hz signal generated by the acoustic signal generator several other frequencies can be seen, mostly in the lower regions of the spectrogram. These becomes more prominent in the later part of the recording when Ägir is close to the array, which indicates that they are generated by Ägir. In the area around 2500 s another vessel temporarily passes the array at a very close distance which reduces the influence of Ägir temporarily.

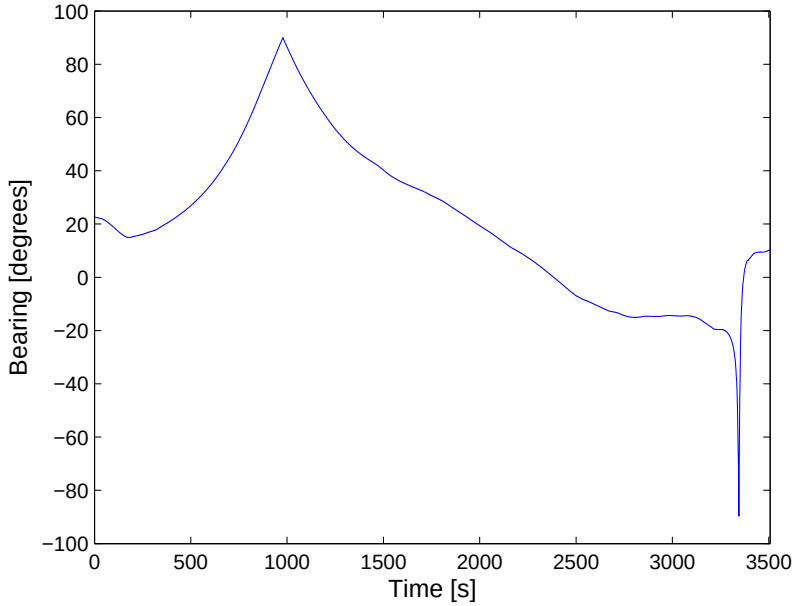

Figure 12: *Bearing curve for the DGPS track to Track 1 in the interval* $[-90°; 90°]$. *Sharp peaks at about* $1000\,s$ *and* $3350\,s$ *represent the moments where the vessel passes the End Fire of the ULA.*

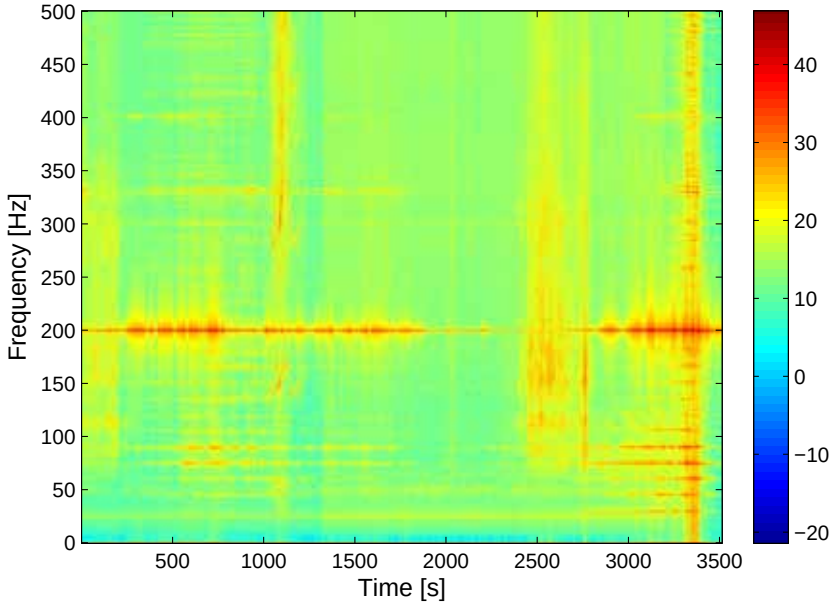

Figure 13: *Spectrogram for Track 1 with a* 1 *s estimation window with no recursive updating of the SCM.*

Track 2

Track 2 is a recording of the vessel Ägir without the towed acoustic signal source RAMSE. In this case the tracking of the vessel has to be performed by searching for frequencies that is created by Ägir. The average velocity is in this case 3.9 *knots* which is almost the same as in *Track 1*. This yields that the signature created by Ägir should be almost the same as in *Track 1* apart from the 200 *Hz* signal. Ägir moves according to the DGPS track in Figure 14 where the location of the used array aperture is marked with a black line.

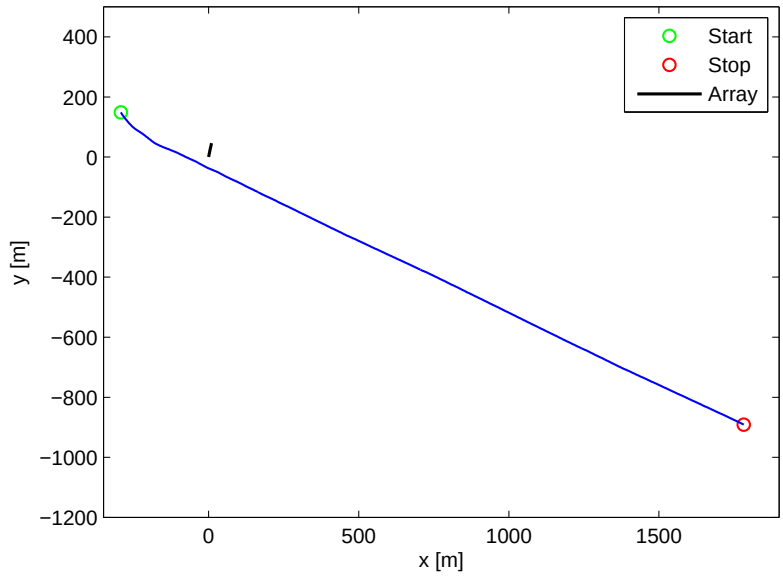

Figure 14: *DGPS track for Ägir in recording Track 2. The black thick line represents the ULA and the green and red circles represent the start and end of the DGPS signal.*

The DGPS track is transformed to bearings relative the linear array in the same manner as for *Track 1*. The received bearing curve from the DGPS track is illustrated in Figure 15. Figure 16 shows the spectrogram obtained for *Track 2* when a 1 *s* estimation window is used. As can be seen, most of the energy for the received signal lies in the lower regions of the spectrogram, approximately around $60 - 100$ Hz. This energy probably correspond to frequencies that are created by Ägir.

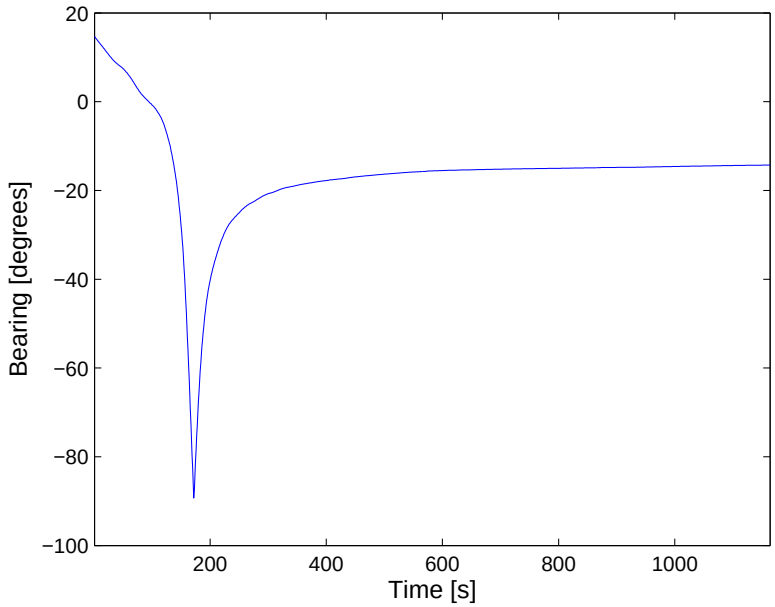

Figure 15: *Bearing curve for the DGPS track to Track 2 in the interval* $[-90°; 90°]$.

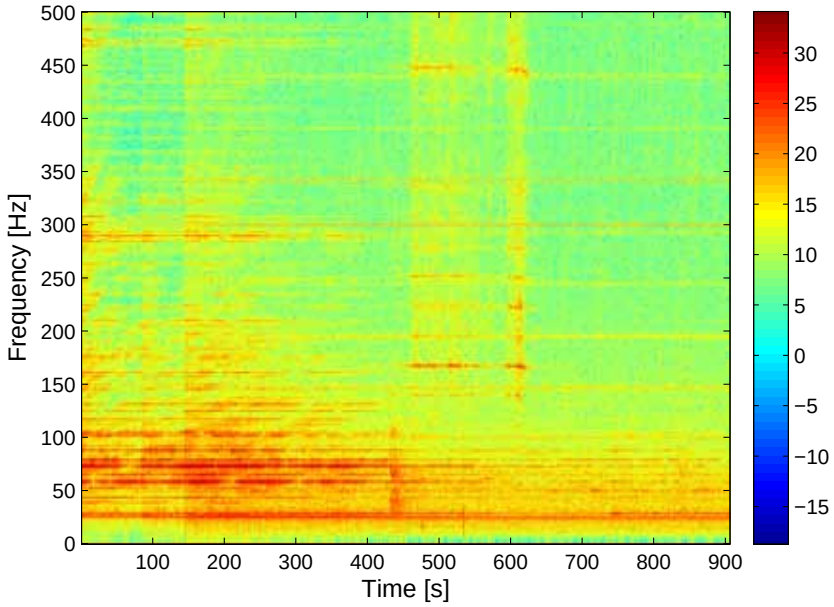

Figure 16: *Spectrogram for Track 2 with a* 1 *s estimation window with no recursive updating of the SCM. Most of the received signal energy lies in the region* $60 - 100$ Hz*. This energy is most likely generated by Ägir.*

Track 3

In *Track 3* there are two vessels present, Ägir and FOI's experiment vessel Decibella. Each vessel is equipped with an acoustic signal source that both emit a 200 *Hz* signal. The source Ramse is towed behind Ägir at a depth of 7 *m* and the source Argotech is towed behind Decibella at a depth of 2.5 *m*. Ägir moves with an average velocity of 4.2 *knots* and Decibella with 2.9 *knots*. The vessels move according to the DGPS pattern in Figure 17, where the position of the array is marked with a black line.

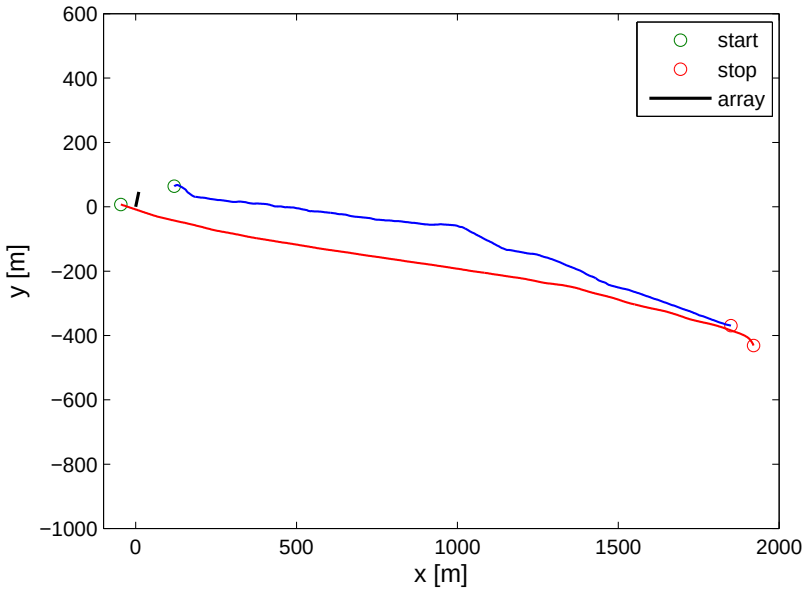

Figure 17: *The figure shows the DGPS patterns for the vessels in recording Track 3. The black thick line represents the ULA and the green and red circles represent the start and end of the DGPS signals. The blue line corresponds to the DGPS pattern for Decibella and the red line corresponds to Ägir.*

The DGPS pattern is transformed to bearings relative the linear array in the same manner as for *Track 1* and *Track 2*. The bearing curves from the DGPS patterns are illustrated in Figure 18.

By analysing the recorded signal in the frequency domain at different moments a time-frequency dependency can be calculated according to the spectrogram in Figure 19. From this spectrogram the most prominent frequencies during the recording can be recognized.

As have been seen for previous tracks the interval $50 - 100$ *Hz* corresponds to the signature from Ägir. Frequencies that corresponds to Decibella's own signature is much harder to find, but it seems like the frequencies are spread out over the entire useable frequency band ($50-450$ *Hz*), compared with the spectrogram in Figure 16 for only Ägir.

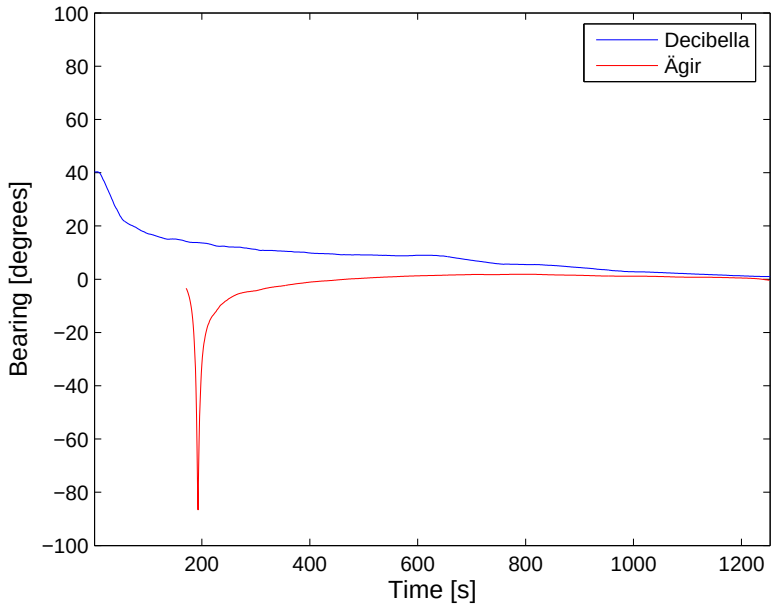

Figure 18: *Bearing curves for the DGPS patterns to Track 3 in the interval* $[-90°; 90°]$.

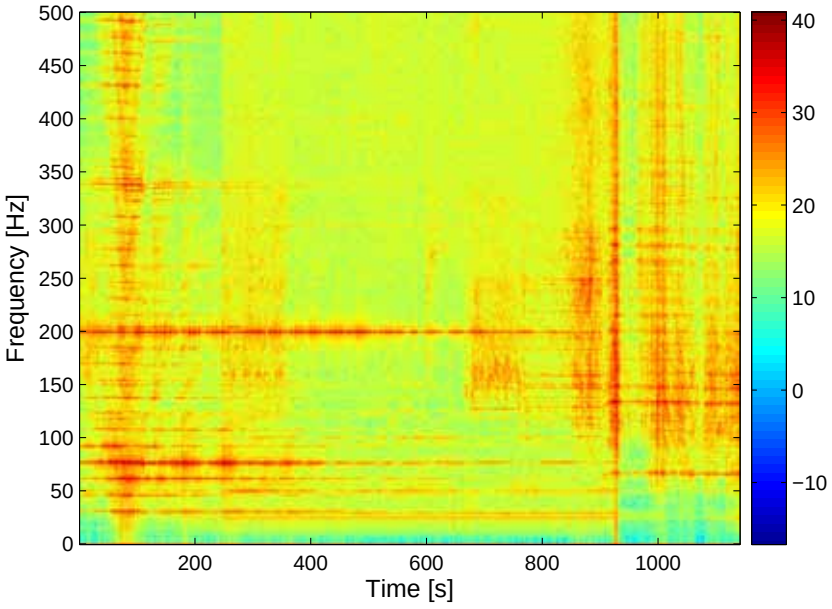

Figure 19: *The spectrogram for Track 3 with a* 1 *s estimation window with no recursive updating of the SCM.*

5 Analysis

This chapter describes the different criteria (Section 5.1) and approaches (Section 5.2) that have been used to evaluate the obtained bearing results (Section 5.4-5.7) from the analyses performed on the tracks described in Chapter 4. Section 5.3 describes with a block diagram the different signal processing steps that have been performed to estimate the bearings.

For *Track 1* the window size and the error analysis are only performed on the first 2200 *s* of the recording. The reason is that after this point another undesired vessel passes the array and temporarily drowns the signal from Ägir. This causes large errors in the tracking of Ägir.

5.1 Criteria for Evaluation of Bearing Algorithm Performance

To examine the performance of different DOA estimation methods and to compare them with each other, they can be evaluated by different criteria. In this thesis resolution, bias and variability (Root Mean Square (RMS) and STandard Deviation (STD)) was taken in consideration.

- Resolution means the ability to resolve the presence of two, closely spaced sources. A sharper spectral peak will imply a better resolution and a more accurate bearing estimate.
- Bias means the accuracy or the error in the position, bearing, of the peak. Higher bias gives a more inaccurate bearing estimate.
- Variability means the range over which the bearing estimates, the spectral peaks, is expected to vary. It can be measured in RMS, STD etc.

Resolution

The resolution properties are dependent on the physical constraints of the array and the signal processing method that is used. The resolution for the different methods is further described in respective section, and therefore only the analytical expressions are shown here. The resolution for CB is expressed as

$$\theta_{CB} = \frac{C\lambda}{L} \tag{38}$$

where L is the physical length of the array ($L = (M-1)d$), M is the number of sensors in the array, λ is the signal wavelength and C is a constant (50.5^o) set by the weights w_n in the steering vector $\mathbf{S}$ (Eq. 12 in Section 3.2). The resolution for MV in radians is expressed as

$$\theta_{MV} \approx \left(\frac{MP_s}{P_n}\right)^{1/4} \frac{\lambda}{L} \tag{39}$$

where $\frac{P_s}{P_n}$ is (SNR). The resolution for MUSIC in radians is expressed as

$$\theta_{MUSIC} \approx \left(\frac{\frac{P_s}{P_n}}{\frac{P_n\gamma^2}{P_sM^2} + \frac{1}{N}}\right)^{1/4} \frac{\lambda}{\widetilde{L}} \tag{40}$$

where γ is an estimate for the spreading of the noise eigenvalues e_i, N is the used window size (number of snapshots) and $\widetilde{L}$ is the synthetic array length (see Eq. 36) that is created by EV and MUSIC (see Section 3.4).

Bias

Bias is a measure of the deviation (offset) in the estimated values from the true values. High bias indicates bad accuracy in the estimate values. The bias is estimated as the mean for the error between the true and estimated bearings according to

$$BIAS = \frac{1}{D}\sum_{n=1}^{D}(x_n - \hat{x}_n) \tag{41}$$

where D is the number of true and estimated values, x_n is the true values and $\hat{x}_n$ is the estimated values.

Variability

Variability is a statistical quantity for the range over which the estimates is expected to vary. Traditionally this range is measured by means of RMS and/or STD. RMS will in this thesis refer to the square root of the mean of the squares of the errors. With error means the dispersion between a true value and an estimated value. The RMS is expressed as

$$RMS = \sqrt{\frac{1}{D}\sum_{n=1}^{D}(x_n - \hat{x}_n)^2} \tag{42}$$

where D is the number of true and estimated values, x_n is the true values and $\hat{x}_n$ is the estimated values. STD is almost the same as RMS and will in good situations give approximately the same value. The difference between them is that STD also consider the mean value (mean error, bias) in the estimation. STD can be expressed in two different ways, but in this thesis only the expression according to Eq. 43 will be used.

$$STD = \sqrt{\frac{1}{D-1}\sum_{n=1}^{D}((x_n - \hat{x}_n) - \overline{x})^2} \quad \text{where}\, \overline{x} = \frac{1}{D}\sum_{n=1}^{D}(x_n - \hat{x}_n) \tag{43}$$

where $\overline{x}$ is the mean error between x_n and $\hat{x}_n$.

5.2 Approaches

To investigate the performance for the three bearing algorithms regarding the RMS, STD and Bias error several different approaches can be used. Possible approaches can be: *Single Frequency Method*, *Maximum Peak Method* and *Mean Power Method*.

1. The *Single Frequency Method* uses only one frequency to estimate the bearings to the source, i.e. it is a narrowband method. The frequency that is used is either chosen directly by the user and is then static during the entire recording, or it is estimated from the frequency spectrum for every estimation window by using the highest peak in the frequency spectrum.
2. The *Maximum Peak Method* is a narrowband method that estimates several frequencies, a frequency band, in the frequency spectrum. The idea is to first estimate the frequency that corresponds to the highest peak in the frequency spectrum. Then set a threshold, where peaks above the threshold are considered as usable frequencies. Each frequency yields a Power-Bearing spectra. The Power-Bearing spectra that have the highest peak is chosen to be representing the desired source. In this way it is perhaps possible to find a good bearing estimate of the DOA even if the used frequency is not corresponding to the highest peak in the frequency spectrum.

3. The *Mean Power Method* uses the same idea with the frequency band as *Maximum Peak Method* but instead of using only the Power-Bearing spectra that corresponds to the highest peak, it uses all Power-Bearing spectras and estimates an average Power-Bearing spectra. The highest peak in this spectra is assumed to correspond to the desired source. The reason for the averaging is to reduce the influence of spurious frequency peaks that can represent noise sources, which some times can be higher than peaks representing true sources. This method can be considered as a more broadband approach.

5.3 Signal Processing

To obtain accurate bearing estimates the received signal has to pass some signal processing steps to remove disturbances, i.e. undesired sources and noise from the media. This has to be done in a manner so that the information about the true source is preserved. The signal processing model used in this thesis is described with the block diagram in Figure 20.

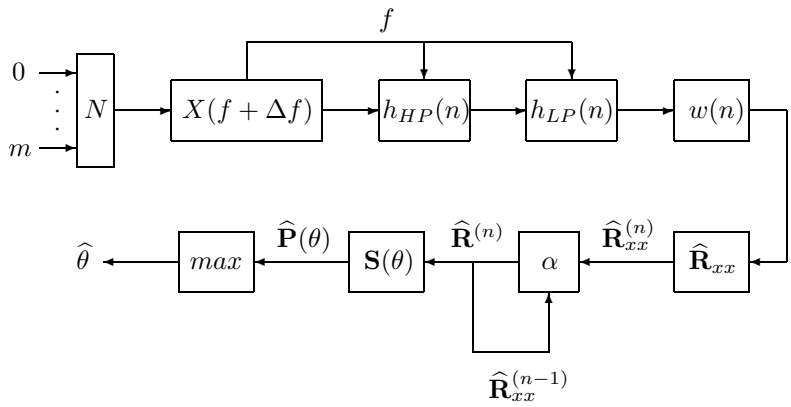

Figure 20: *Block diagram of the different signal processing steps that are performed between received signal and estimated bearing.*

The signal is received at the M sensors in the array, with a time difference between the sensors dependent on the bearing. When enough signal data are received at each sensor, the blocks of data are sent forward to be processed. Each data block, or estimation window, has a length N (number of snapshots).

The first step is to find out which frequency or frequencies that are most characteristic for the received signal and which maybe correspond to the signature of the vessel. This is done by first estimating the FFT to the block on the reference sensor and then searching for the highest peak/peaks in the frequency spectrum. The FFT is only performed for estimation of the frequency/frequencies. The signal that is used in later parts of the signal processing is still the received time-domain signal. The frequency resolution, or the accuracy in the frequency estimate, is dependent on the used block length N and the sampling frequency f_s as

$$\Delta f = \frac{f_s}{N}.$$

If for example $N = f_s$ the resolution Δf is 1 *Hz*. If more than one frequency is used (see Section 5.2), the chosen frequencies has to be separated at least with 20 *Hz* to be considered

as new frequencies and not side lobes to the adjacent frequency. This is also dependent on the filter settings, see below. The frequencies are chosen in a decreasing order with the strongest frequency first. The maximum number of frequencies that are used is limited to 5. The chosen frequencies are required to be in the interval $50 - 450$ *Hz*. Frequencies above 500 causes aliasing with the used array configuration according to the spatial sampling theorem described in Section 2.3.2.

The next step is to filter the data blocks to reduce undesired information that can inflict on the bearing estimation and give bad accuracy in the estimates. Each block is first high pass filtered and then low pass filtered, both centered around the estimated frequency. This is done to improve the SNR and to avoid false bearing information. Both filters are *4th* order Butterworth filters with cut-off frequencies set to $f \pm 20$ *Hz*. The width of the filter is set to avoid instability. The reason for the low pass and high pass filtering instead of a direct bandpass filtering is that the edges of the filter can be made steeper with the same order on the filters. By keeping the order low the risk of unstable filters is avoided. This approach is however a little bit slower.

When the signal is divided into rectangular blocks a truncation at the borders of each block is introduced. This truncation can be rectified by making a time-domain filtering, windowing, on each block. In this thesis a Hanning window is used for this purpose.

Next is to estimate SCM. The first objective is to make the SCM estimate unbiased, which is done by subtracting the mean value from each block. Then the SCM can be estimated in the time domain according to Eq. 7 in Section 3.1. One problem that occurs when estimating the SCM in the time domain is that the estimate will be real, not complex, if the received signal is real, as it is in our case. To be of any use, the estimated SCM has to be complex (i.e. analytic) which can be done by using the Hilbert transform described in [15], page 618 (function *HILBERT* in Matlab). To improve the bearing accuracy and avoid bad estimates of the SCM, the SCM is recursively updated between every bearing estimate according to Eq. 8 in Section 3.1.

The final step is to estimate the bearing to the source using any of the described bearing methods in Section 3.2-3.4. To find the bearing, the power $\mathbf{P}$ of the beam is estimated in every direction that the array is steered in. In this way, the power $\mathbf{P}$ becomes a function of the direction. The directions that are considered are uniformly separated by 0.5 degrees in the interval $[-90; 90]$ degrees. The direction that yields the highest value for $\mathbf{P}$ is assumed to be the direction of the source.

5.4 Window Size Analysis

The first issue to be considered is to find an appropriate length of the estimation window that optimizes the accuracy in the bearing estimates. The length of the estimation window is evaluated with regard to the condition number of the SCM and the error deviation between the DGPS bearing and the estimated bearing, which is measured in RMS, STD and bias error.

5.4.1 Spatial Covariance Matrix Properties

The SCM carries the information about the intersensor correlation and the phase difference that is used in the estimation of the bearing. The size of the window affects the information accuracy and generally a longer window results in more accurate information, dependent on the stationarity time for the received signal. The properties of the SCM were discussed in Section 3.1.

Some issues that limit the length of the estimation window are the required computational time, the time resolution (e.g. a longer window gives a decreased time resolution and longer time delay between the bearing estimates) and the time-lagging between the estimated bearing and the source present position (i.e. the estimated bearing represents a direction where the source was some time ago). A lower time resolution results in poor tracking of a moving source, which can have major consequences if the source is moving fast with short bearing stationarity. If the source is moving relatively slowly (i.e. the signal has relatively long stationarity time), the size of the window is less important, and a long window can be chosen without major loss of accuracy. Time-lagging is an important aspect to consider if the task is to track (follow) the source in real-time.

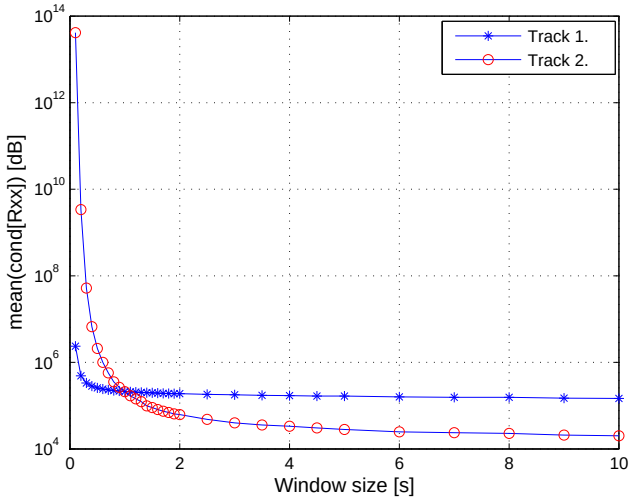

Figure 21: *Illustration of the relationship between the length on the estimation window and the condition number for the SCM* $\mathbf{R}_{xx}$ *for Track 1 and Track 2. The condition number for each window size is marked with a blue* $*$ *for Track 1 and a red* $\circ$ *for Track 2. The used sampling frequency is* $f_s = 25\ kHz$.

Figure 21 shows the relationship between the length of the estimation window (expressed in seconds) and the mean condition number of the SCM for *Track 1* and *Track 2*. As can be seen in the figure an increased length of the estimation window yields a better condition number for both tracks. The length of the estimation window is chosen from the point where the relative change of the condition number is small (i.e. choosing a longer estimation window will not result in better condition number). For *Track 1* this point occurs at approximately $0.5 - 1\ s$ and for *Track 2* it is approximately $2 - 6\ s$. See Section 3.1 for further information about the condition number.

5.4.2 Error Analysis

Figures 22-24 show the estimated global RMS, STD and bias errors as functions of the length of the estimation window, for CB (part A), MV (part B) and MUSIC (part C) for *Track 1*. In each part the global RMS, STD and bias errors have been estimated for all three approaches *single frequency method*, *maximum peak method* and *mean power method*, see Section 5.2. For the *single frequency method* the used frequency f is set to 200 Hz during the entire recording.

For *maximum peak method* and *mean power method* the used frequencies are estimated from the frequency spectrum.

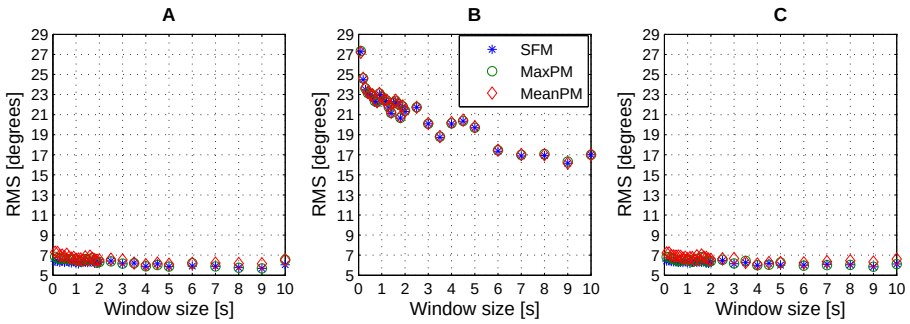

Figure 22: *Part **A** shows the global RMS errors obtained with CB, part **B** for MV and part **C** for MUSIC, for Track 1. The RMS errors are estimated for all three approaches (SFM - Single Frequency Method, MaxPM - Maximum Peak Method, MeanPM - Mean Power Method).*

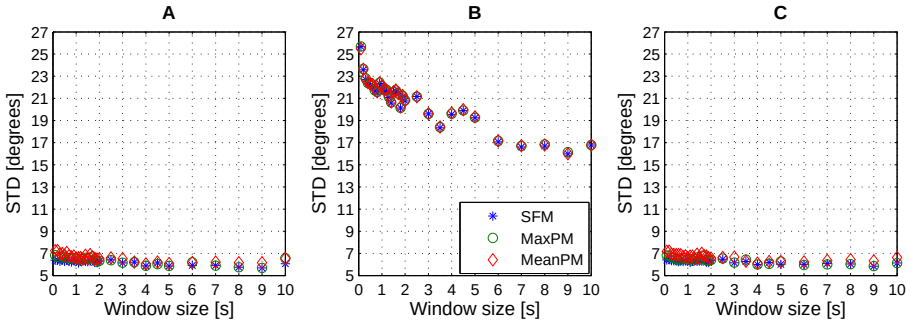

Figure 23: *Part **A**, **B** and **C** as in Figure 22 for the STD of the errors.*

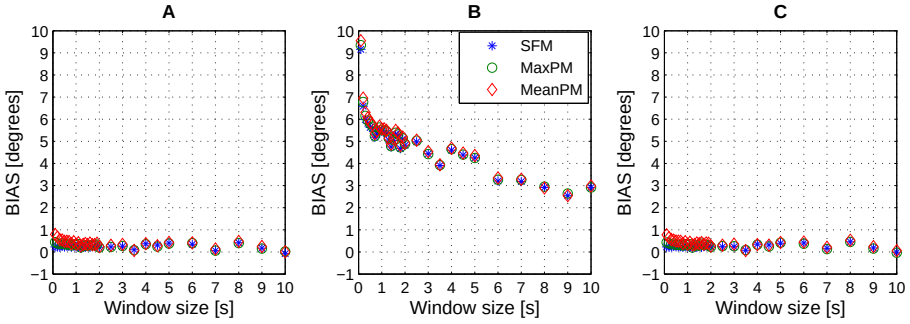

Figure 24: *Part **A**, **B** and **C** as in Figure 22 for the bias errors.*

Figures 25-27 show the estimated global RMS, STD and bias errors as functions of the length of the estimation window, for CB (part A), MV (part B) and MUSIC (part C) for *Track 2*. In each part the global RMS, STD and bias errors have been estimated for all three approaches *single frequency method*, *maximum peak method* and *mean power method*, see Section 5.2. In this case the frequency f is estimated for the *single frequency method* as for the other approaches.

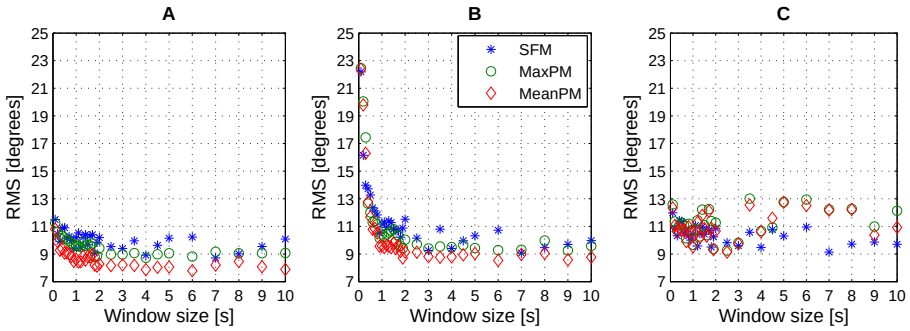

Figure 25: *Part* ***A*** *shows the global RMS errors obtained with CB, part* ***B*** *for MV and part* ***C*** *for MUSIC, for Track 2. The RMS errors are estimated for all three approaches (SFM - Single Frequency Method, MaxPM - Maximum Peak Method, MeanPM - Mean Power Method).*

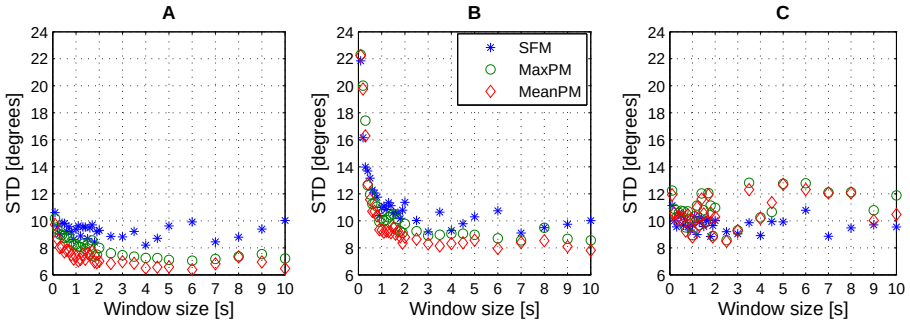

Figure 26: *Part* ***A****,* ***B*** *and* ***C*** *as in Figure 25 for the STD of the errors.*

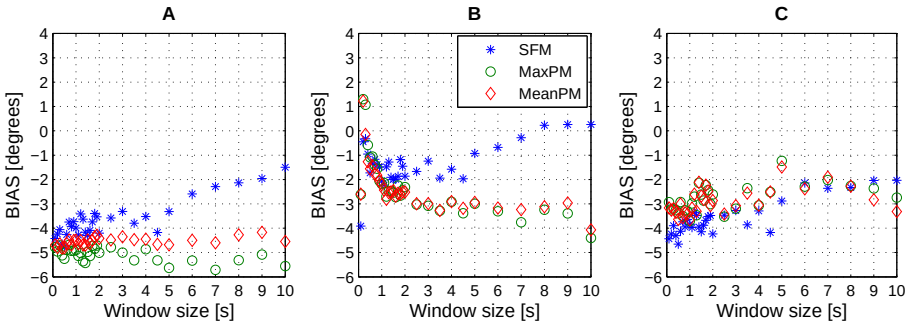

Figure 27: *Part* ***A****,* ***B*** *and* ***C*** *as in Figure 25 for the bias errors.*

For the MUSIC algorithm the number of sources p has to be set in some way, either static or estimated with the method described in Section 3.5. For *Track 1* the signal from the source is very strong with a clear frequency, see spectrogram in Figure 13, Section 4. Therefore p is set to 1 during the entire measurement for all three approaches. The bearing performance for MUSIC was also evaluated when p was estimated. However, it was shown to have almost the same bearing performance. For *Track 2* p is set to 1, given by the small differences in the bearing performance. The estimated number of p for both tracks is shown in Figure 28.

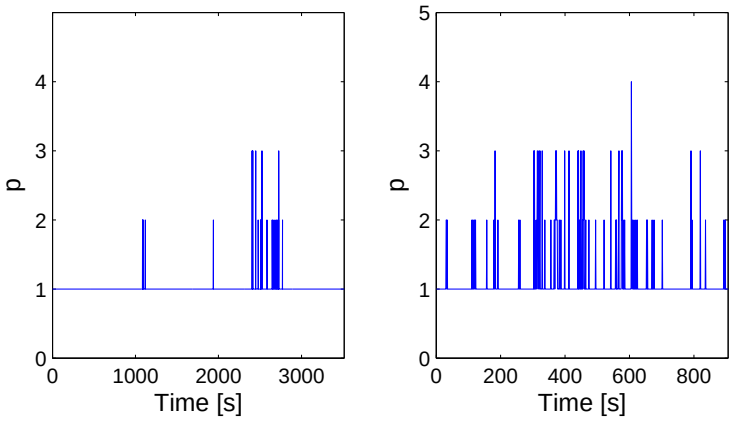

Figure 28: *Estimated number of sources p for Track 1 (left figure) and Track 2 (right figure) using the gradient method described in Section 3.5. As can be seen the estimated p differs from the true p (1) more in Track 2. During this track the vessel was not equipped with an acoustic signal generator as in Track 1.*

From the error analysis performed on *Track 1* no distinct optimal value for the length on the estimation window can be obtained for either bearing algorithm. Although, for CB and MUSIC the performance is almost constant, with a small improvement for longer estimation windows. This indicates that a fairly short estimation window can be chosen, without losing bearing performance. The RMS error and the STD of the error for both CB and MUSIC is approximately the same for all sizes on the estimation window. This comes as a result of the low bias in the bearing estimates. For MV the bearing performance is far worse than for CB and MUSIC, but is improved with a longer estimation window. This difference in bearing performance is presumably dependent on that MV, unlike CB and MUSIC, uses the inverse of the SCM in the bearing estimation (see Section 3.3). The inverse of the SCM seems to require better ambient conditions and that the noise is isotropic (see noise assumption in Section 2.3.2) to give accurate bearing estimates. The bearing accuracy can presumably be increased by either using diagonal loading of the SCM to prevent singularity or by using pre-whitening of the signal before SCM estimation (see [16], pages 139-140, or [15], Section 11). For all three used bearing algorithms the *single frequency method* is shown to have a slightly better bearing performance than the two other used approaches.

The error analysis performed on *Track 2* does not give any indication about the optimum value for the length on the estimation window. One difference from the analysis on *Track 1*, is that MV seems to work better for *Track 2*. The bearing performance is almost the same for MV, as for CB and MUSIC, for estimation windows longer than 0.5 *s*. In this track the *mean power method* works slightly better than the *single frequency method* and the *maximum peak method*. This is presumably a result of that the vessel has a signature that consists of several strong frequencies. By using several frequencies that originate from the source the performance is in

this case improved.

5.5 Recursive Updating Analysis

As seen in Section 5.4 one way to improve the accuracy in the bearing estimates is to increase the length of the estimation window with respect to the stationarity time of the signal. In many applications the length of the estimation window is limited by e.g. required computational time, time-lagging or time resolution etc. Therefore, it is necessary to find other methods that improve the bearing performance.

This section evaluates the bearing algorithms performance when the SCM is recursively updated between every bearing estimate. Recursive updating means that parts of the previous received data blocks are reused along with the present received data block in the estimation of the SCM. The objective with recursive updating is to avoid poor estimates of the SCM by using data from previous, hopefully better SCMs and in that way improve the bearing performance. The amount of reused data is determined by the value of α. Recursive updating can be seen as a method to artificially create a larger estimation window, where α determines the size, without obtaining the drawbacks of time-lagging etc. Further information about the recursive updating and used equations can be found in Section 3.1.

The results obtained with the recursive updating are evaluated with regard to the condition number of the SCM and the error deviation between the DGPS signal and the estimated bearings, measured in RMS, STD and bias. The updating constant α can be chosen in many ways, where the two approaches below are evaluated in this thesis.

1. *Static updating*: α is set static during the entire recording.
2. *SNR dependent updating*: α is chosen from the SNR level.

The recursive updating process is performed and evaluated on some of the sizes on the estimation window evaluated in the previous section. The sizes are chosen to be the same for all three bearing algorithms even if the performance has been shown to be different for each algorithm. The reason for this is to see if recursive updating is better to use when the bearing performance is bad, instead of increasing the length of the estimation window. The chosen sizes on the estimation window are 0.5, 1.0, 2.0 and 5.0 s. Furthermore, the results of the recursive updating will only be shown for the *single frequency method* described in Section 5.2, since the other two described methods have similar behaviour. For *Track 1* the frequency is set static to 200 Hz and for *Track 2* the frequency is estimated from the frequency spectrum. For both tracks the MUSIC algorithm has p set to 1, see Section 5.4.2.

5.5.1 Static Updating

Spatial Covariance Matrix Properties

Figures 29 and 30 show the condition number for the estimated SCM as a function of α, for the chosen sizes on the estimation window 0.5, 1.0, 2.0 and 5.0 s respectively, for *Track 1* and *Track 2*.

From the condition number analysis performed on *Track 1* shown in Figure 29, no distinct optimal value for α can be obtained for any used size on the estimation window. As can be seen the condition number of the SCM improves with a decreasing value on α for all four evaluated sizes of the estimation window. This indicates that a smaller value on α is more

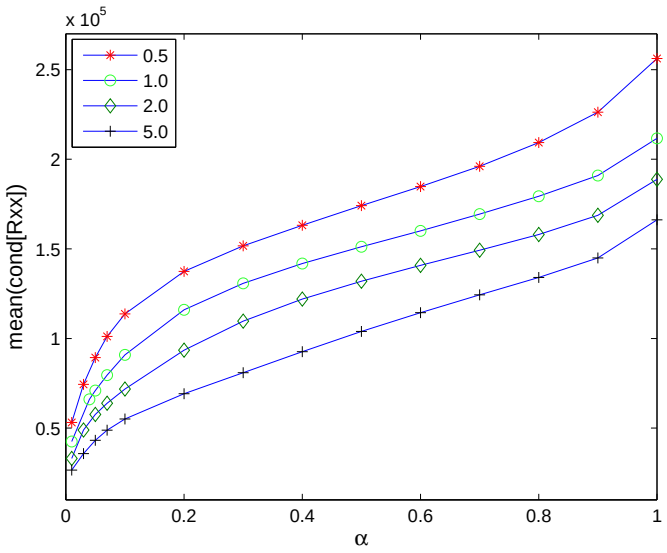

Figure 29: *The condition number cond*($\mathbf{R}_{xx}$) *for the estimated SCMs as a function of* α *for the used window sizes* 0.5, 1.0, 2.0 *and* 5.0 *s, for Track 1. Every condition number is the average condition number for the entire recording, for each* α *value.*

preferable. For *Track 2* the condition number analysis shown in Figure 30 is more rewarding, and an optimal value for α can be found. The optimal value on α is shown to be dependent on the size on the estimation window where a larger size on the estimation window has a larger value on α. This verifies the discussion in the introduction to Section 5.5 that the value on α determines the length of an artificially created estimation window. A too long artificial estimation window will have a decreased bearing performance dependent on the stationarity time of the received signal, and this point of deceasing will occur at different α values dependent on the size of the estimation window. The found optimal values on α are 0.03, 0.07, 0.1 and 0.3 respectively for the 0.5, 1.0, 2.0 and 5.0 *s* estimation windows.

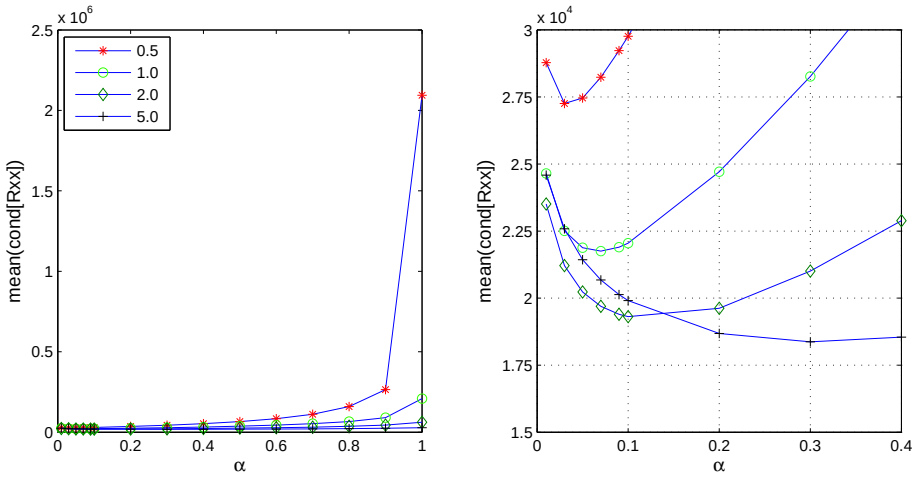

Figure 30: *The left figure shows the condition number cond*($\mathbf{R}_{xx}$) *for the estimated SCMs as a function of* α *for all used window sizes* 0.5, 1.0, 2.0 *and* 5.0 *s, for Track 2. Every condition number is the average condition number for the entire recording for the specific used* α *value. For this track the condition number analysis indicates that an optimal value for* α *exists, and it will be dependent on size on estimation window. The right figure shows the segment where the optimal values on* α *are.*

Error Analysis - Track 1

The analysis made on the RMS, STD and bias errors for all three bearing algorithms shows that there is an optimum for α for *Track 1*, and it is dependent on the length of the estimation window. The optimum α are approximately the same for all three bearing algorithms. The found optima on α are approximately 0.03, 0.05, 0.1 and 0.2 for the estimation windows 0.5, 1.0, 2.0 and 5.0 *s* respectively. This is shown in Figures 31-33.

By performing the error analysis on *Track 1*, optimums on α have been obtained which are similar to the optimums obtained for *Track 2* shown in Figure 30. This similarity indicates that the obtained optimal α values are valid. The reason for the decreased bearing performance for α smaller than the optimum, is that the signal can not be considered stationary anymore as a consequence of the artificially increased window length (see the window size analysis in Section 5.4.2). The decreased bearing performance for larger values on α are depending on poor SCM estimates.

As can be seen in Figures 31-33 the bearing performance is increased for all evaluated sizes on the estimation window. The performance will almost be the same for each length on the estimation window when used together with its optimum on α. This shows that the recursive updating of the SCM is a better solution to obtain good bearing performance instead of increasing the size on the estimation window, and thereby introducing time-lagging and longer computational time (see Section 5.4).

Both CB and MUSIC have a similar increase in the bearing performance with the recursive updating of the SCM. The bearing performance, regarding RMS and STD, is almost at a constant level for large values on α, but the performance increases substantially close to the optimum on α. The bias is almost 0 for both algorithms for α values larger than the optimum. For α values smaller than the optimum, the bias differs from 0.

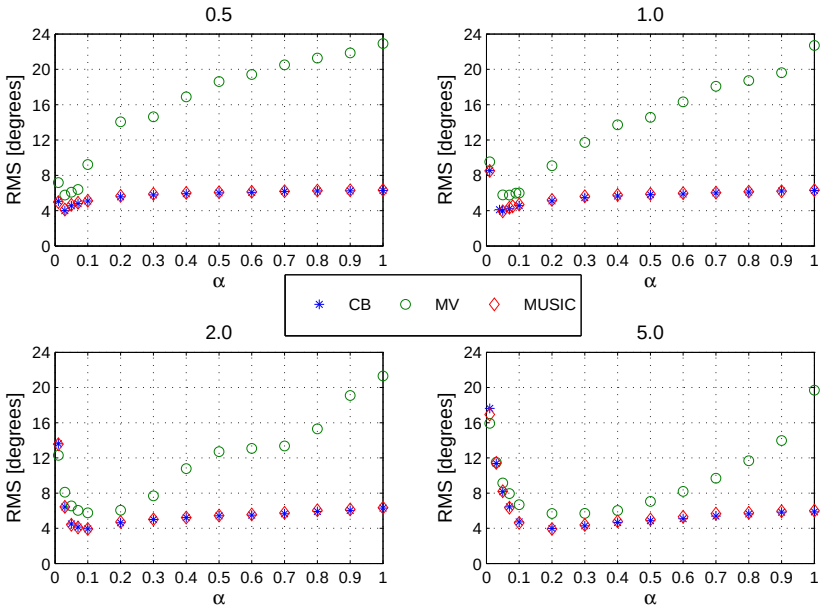

Figure 31: *RMS error for Track 1 for all three bearing algorithms (CB - blue ∗, MV - green o, MUSIC - red diamond) with all evaluated sizes on the estimation window.*

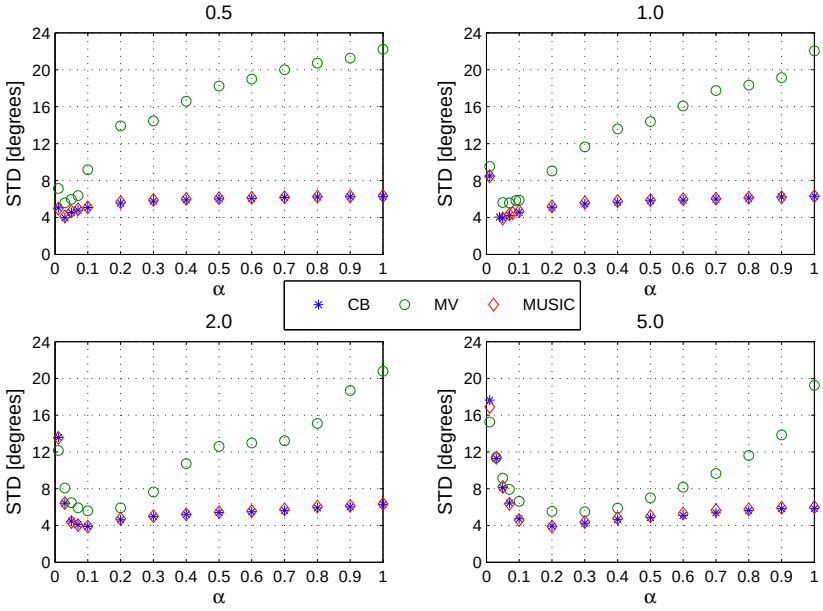

Figure 32: *STD of the error for Track 1 for all three bearing algorithms (CB - blue ∗, MV - green o, MUSIC - red diamond) with all evaluated sizes on the estimation window.*

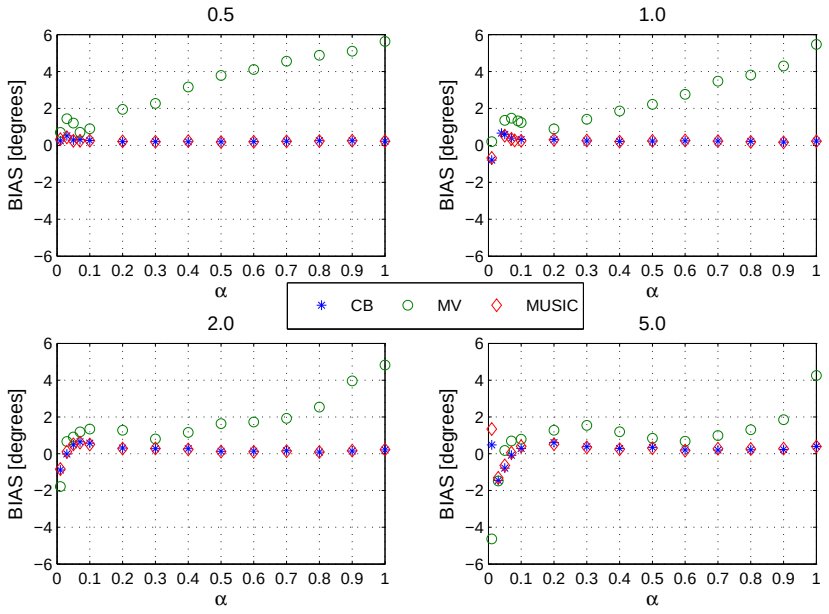

Figure 33: *Bias error for Track 1 for all three bearing algorithms (CB - blue ∗, MV - green o, MUSIC - red diamond) with all evaluated sizes on the estimation window.*

For MV the bearing performance is far worse than for CB and MUSIC, but it increases substantially with the recursive updating of the SCM. At the optimal α value the bearing performance is approximately the same for MV (a little bit worse) as for CB and MUSIC. The improvement for the MV algorithm really shows the benefits of using recursive updating of the SCM to gain better bearing performance.

Error Analysis - Track 2

The results from the error analysis performed on *Track 2* shown in Figures 34, 35 and 36 give no direct indication about the optimal value on α for the different window sizes, as the case were in *Track 1*. The bearing performance increases with smaller α values without a global minimum. This behaviour on α is due to that the movement of the vessel in *Track 2* is almost at constant bearing when it moves away from the array. Therefore will the estimated SCMs in the beginning of the measurement as well as at the end of the measurement yield almost the same bearing. This gives that the system can use a lot of old data (i.e. large memory) in the bearing estimation without obtaining the stationarity effects, like in the case were for *Track 1*.

It should be mentioned that a minimum for α occurs for the 5 *s* estimation window. But this value on α is so small that it can not be considered trustworthy and useful in a more realistic scenario, e.g. *Track 1*. This value will therefore be neglected.

For *Track 2* all three bearing algorithms have a similar bearing performance, regarding the RMS and the STD errors. The bias is improved with a longer estimation window and is better for MV than for both CB and MUSIC which have similar bias levels. Compared with *Track 1* the bearing performance is overall decreased for *Track 2* where there is no 200 *Hz* signal generator present, see Chapter 4.

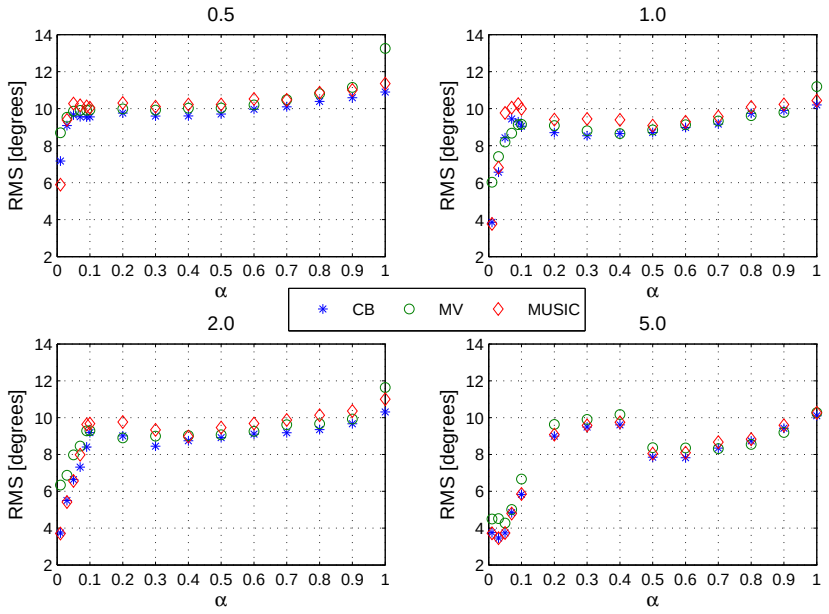

Figure 34: *RMS error for Track 2 for all three bearing algorithms (CB - blue ∗, MV - green o, MUSIC - red diamond) with all evaluated sizes on the estimation window.*

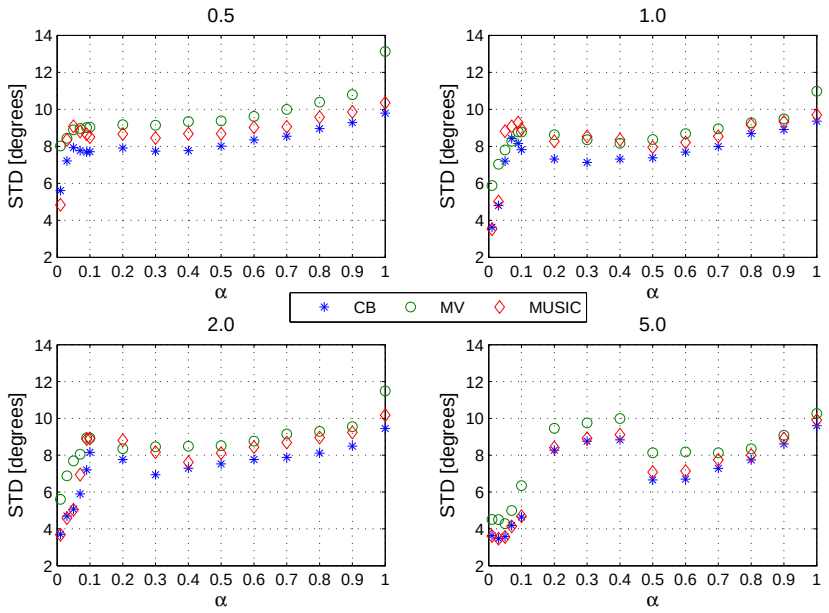

Figure 35: *STD of the error for Track 2 for all three bearing algorithms (CB - blue ∗, MV - green o, MUSIC - red diamond) with all evaluated sizes on the estimation window.*

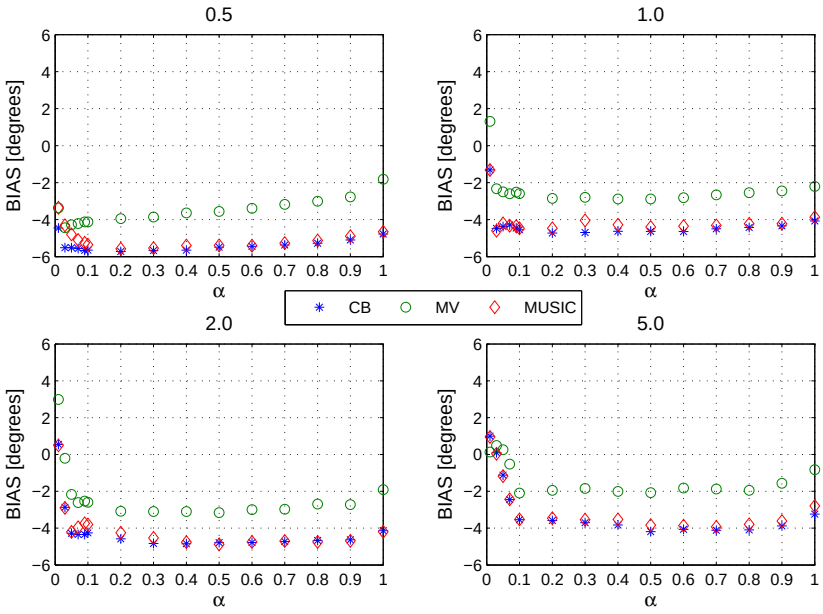

Figure 36: *Bias error for Track 2 for all three bearing algorithms (CB - blue ∗, MV - green o, MUSIC - red diamond) with all evaluated sizes on the estimation window.*

5.5.2 SNR Dependent Updating

The condition of the water between the signal source and the array is time-dependent and differs from one point to another due to signals from other vessels, multipath propagation, temperature or/and pressure etc. It can therefore be convenient to adapt the recursive updating process, i.e. the choice of α, to the changes of the media, and by that means maybe improve the bearing performance. One parameter that can be used for this task is the SNR which is changing over time. Figure 37 shows the estimated SNR for *Track 1* and *Track 2*. The SNR is estimated by calculating the energy from the highest peak in the frequency spectrum and then divide with remaining energy in the spectrum. The spectrum is limited to the interval $50 - 450$ *Hz*.

The SNR for *Track 1* is also shown for the part after 2200 *s*. As can be seen the other vessel cause a large decrease in the SNR.

There are many different methods for adapting the value on α to the SNR. A number of methods have been evaluated, where the method described in Eq. 44 yielded the best bearing performance and was also fairly easy to implement. The method is expressed as

$$\alpha_n = \left(\frac{SNR_n}{SNR_n + SNR_{n-1}} + 0.5 \right) \alpha_{n-1} \tag{44}$$

with initial values $SNR_0 = 20$ *dB* and $\alpha_0 = 0.1 \cdot T$ where T is the size of the estimation window in seconds. The reason for the division between the present SNR and the summation of the present SNR and the previous SNR, is that there in this way will be a smoother change of the estimated α value when the SNR changes. This has been shown to yield better bearing performance. In the situation when the present SNR is approximately the same as the previous

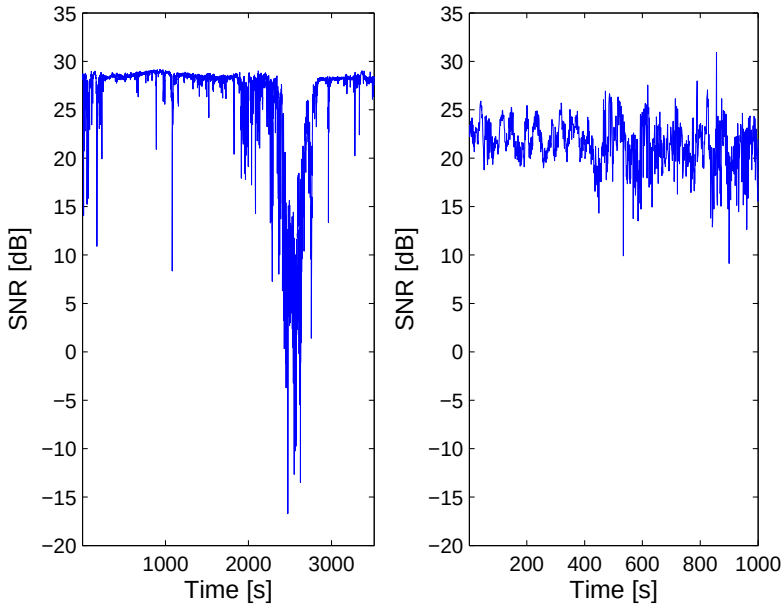

Figure 37: *Estimated SNR for Track 1 (left figure) and Track 2 (right figure).*

SNR the new estimated α should be the same as the previous α. The division factor will in this case be approximately 0.5, which explains the addition of 0.5 in the equation.

Figures 38 and 39 show the estimated global RMS, STD and bias errors with the SNR dependent updating method for *Track 1* and *Track 2*. The errors are plotted as functions of the length on the estimation window.

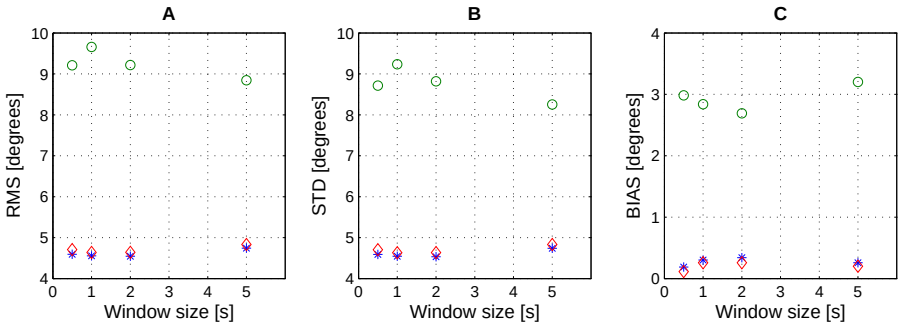

Figure 38: *Estimated RMS, STD and bias errors for CB (blue $*$), MV (green o) and MUSIC (red diamond) for Track 1 using the SNR dependent updating method.*

The bearing performance for *Track 1* is approximately the same for this recursive updating method as for the static updating method described in Section 5.5.1 for CB and MUSIC. For MV the performance is substanially decreased compared with the static updating method. For *Track 2* the bearing performance is approximately the same as for the static updating method.

This method to recursively update the SCM based on the SNR is a non-complicated method.

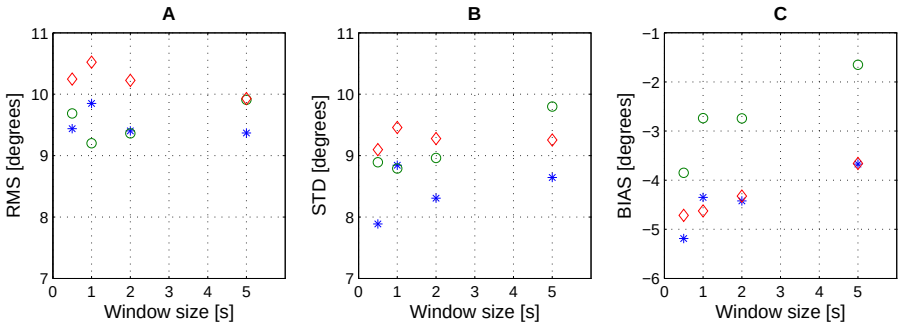

Figure 39: *Estimated RMS, STD and bias errors for CB (blue ∗), MV (green o) and MUSIC (red diamond) for Track 2 using the SNR dependent updating method.*

Perhaps by using a more adaptive and complex SNR based method the bearing performance can be improved. In *Track 1* the bearing performance seems to have reached its peak and it may not be possible to improve it any further using any method. In *Track 2* it has already been shown that the bearing performance can be improved which supports the finding of a better SNR based method than the used one.

5.6 Time-Bearing Images

In all of the evaluated bearing algorithms the procedure to estimate a bearing is to mathematically simulate a steering of the array in different directions. In this thesis the directions are uniformly separated with 0.5° in the interval $[-90° : 90°]$. By estimating the power $\mathbf{P}$ in all directions, a Power-Bearing spectra can be created where $\mathbf{P}$ is a function of the bearing θ. The bearing that gives the highest value on $\mathbf{P}(\theta)$ is assumed to be the bearing of the source. During a recording several Power-Bearing spectra are estimated which can be used to create a Time-Bearing image. The Time-Bearing image illustrates the vessel movement during a recording and is built up by using the Matlab function *imagesc()*. Each spectra has to be normalized to give a clear image of the movement. This is done by setting the highest value in each spectra to 1 and the lowest value to 0. To illustrate the magnitude in the image a colour scale is used where a dark red colour illustrates a high magnitude and a dark blue colour illustrates a low magnitude.

Track 1

Figures 40-42 show the obtained Time-Bearing images for CB, MV and MUSIC on *Track 1* using the *single frequency method*. The SCM is recursively updated with the static updating method described in Section 5.5.1 with $\alpha = 0.07$. The estimation window has a length of 1 s and p is set to 1 for the MUSIC algorithm. As a reference for the estimated bearings, the GPS position of Ägir is plotted with a yellow dashed line.

As can be seen in Figure 40 the tracking of Ägir works well and follows the GPS signal in the beginning of the recording. At about 2300 s the bearing performance is tremendously decreased for some reason. By listening to the received signal it has been found that one other vessel passes the array at a very close distance. The signal from the other vessel drowns the signal from Ägir, which causes a temporary error in the bearing estimation. At about 2800 s the other vessel is far enough from the array and the signal from Ägir is again the strongest one. From this point onwards a small bias in the bearing estimate is introduced compared with

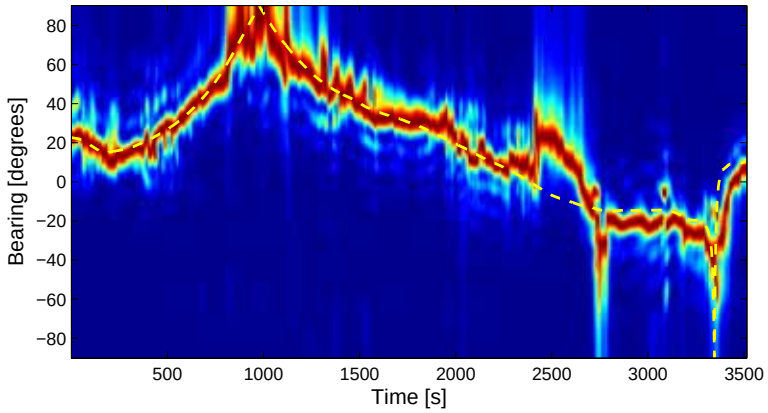

Figure 40: *Time-Bearing spectra for Ägir in Track 1 using CB with the single frequency method. The SCM is recursively updated using a static α value, $\alpha = 0.07$, where the length on estimation window is set to 1 s.*

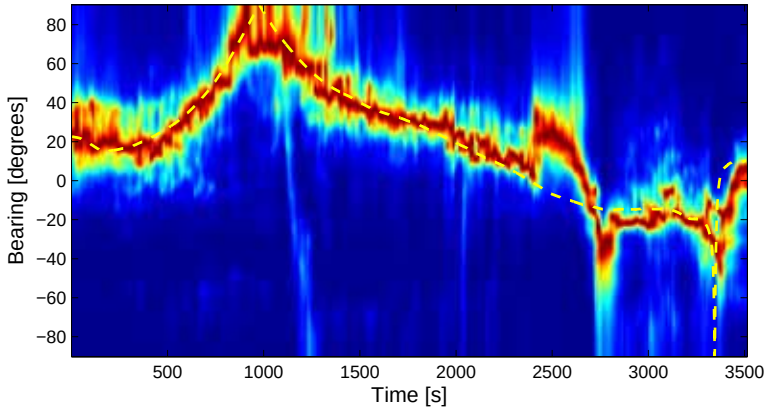

Figure 41: *Time-Bearing spectra for Ägir in Track 1 using MV with the single frequency method. The SCM is recursively updated using a static α value, $\alpha = 0.07$, where the length on estimation window is set to 1 s.*

the GPS signal. At this moment Ägir is very close to the array. The signal generator is towed behind Ägir which has an offset to the GPS signal, which cause a bias in the estimate. This bias error is more noticeable at a small distance. If the beam is steered towards a frequency that is generated by Ägir, this bias can be reduced. The problem is that such a frequency is much weaker than the 200 *Hz* signal, which means that we have to know and lock the steering vector on these frequencies. If these frequencies are used during the entire recording instead of the 200 *Hz* signal the bearing performance is substantially reduced.

If the Time-Bearing images for *Track 1* are compared with each other it can be seen that the MUSIC algorithm has the best resolution, i.e. sharpest main lobe, of the three. The MV algorithm seems to suffer from high side lobe levels and a broad main lobe, which can be due to multipath propagation. This can be one reason why the MV algorithm has a worse bearing performance than both CB and MUSIC.

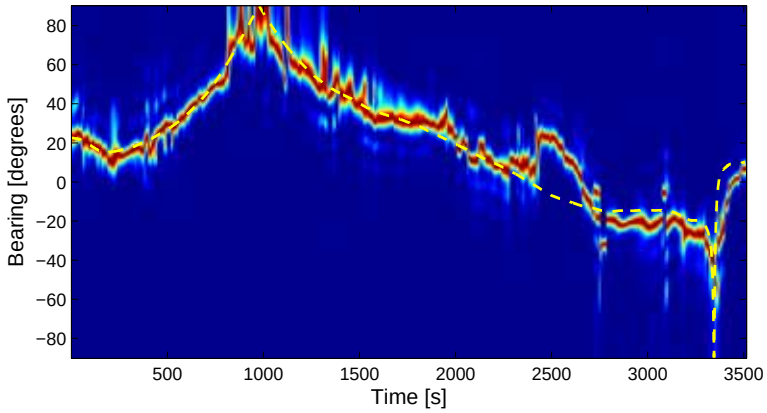

Figure 42: *Time-Bearing spectra for Ägir in Track 1 using MUSIC with the single frequency method. The SCM is recursively updated using a static α value, $\alpha = 0.07$, where the length on estimation window is set to 1 s. p is set to 1.*

Table 1 shows the estimated RMS, STD and bias errors for CB, MV and MUSIC in Figure 40-42. The errors are estimated only on the 2200 first s of the recording.

Table 1: *RMS, STD and bias errors for Track 1 using a 1 s estimation window with static recursive updating of the SCM, $\alpha = 0.07$.*

	RMS, [°]	STD, [°]	Bias, [°]
CB	4.01	3.98	0.50
MV	5.78	5.58	1.48
MUSIC	4.15	4.13	0.44

Track 2

Figures 43-45 show the obtained Time-Bearing images for CB, MV and MUSIC on *Track 2* using the *single frequency method*. The SCM is recursively updated with the static updating method described in Section 5.5.1 with $\alpha = 0.07$. The estimation window has a length of 1 s and p is set to 1 for the MUSIC algorithm. As a reference for the estimated bearings, the GPS signal to Ägir is plotted with a yellow dashed line.

Even though Ägir is not equipped with an acoustic signal generator the tracking works very well, for all three bearing algorithms, especially for the MUSIC based algorithm. From 600 s and onwards a small bias error is introduced, which can be caused by other vessels passing the array.

The main lobe in this track is much broader, i.e. the resolution is decreased, compared to the main lobe in *Track 1*. This is because of the lower the frequencies used for the tracking of Ägir in this track. This yields broader main lobes and thereby a decreased resolution. In this case the frequencies used in Ägirs signature lies in the interval $60 - 100$ *Hz*. As can be seen in Figures 43-45 the resolution for MUSIC is much better than for both CB and MV.

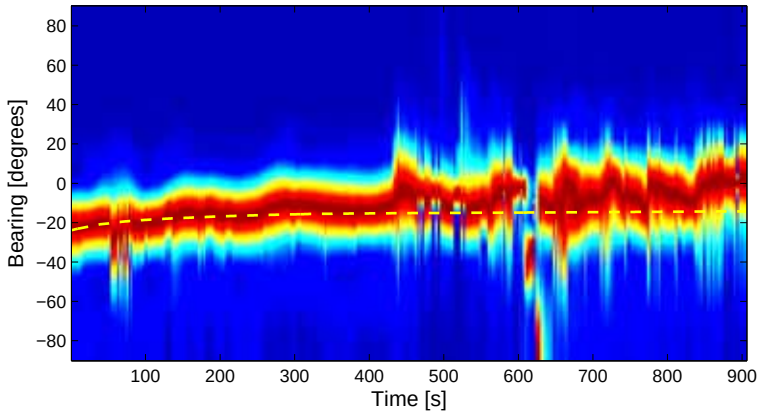

Figure 43: *Time-Bearing spectra for Ägir in Track 2 using CB with the single frequency method. The SCM is recursively updated using a static α value, $\alpha = 0.07$, where the length on estimation window is set to 1 s.*

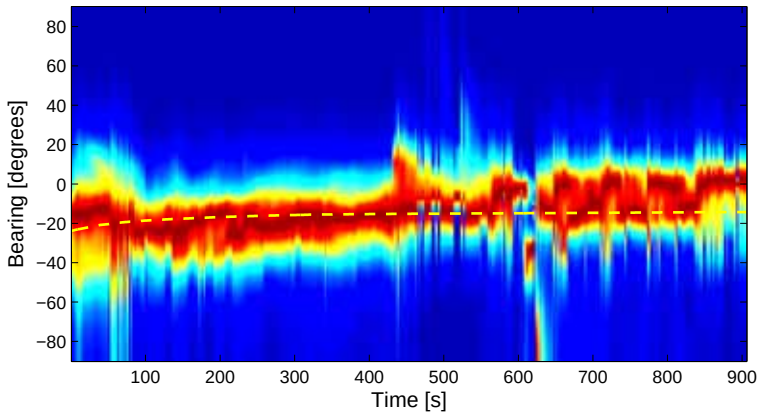

Figure 44: *Time-Bearing spectra for Ägir in Track 2 using MV with the single frequency method. The SCM is recursively updated using a static α value, $\alpha = 0.07$, where the length on estimation window is set to 1 s.*

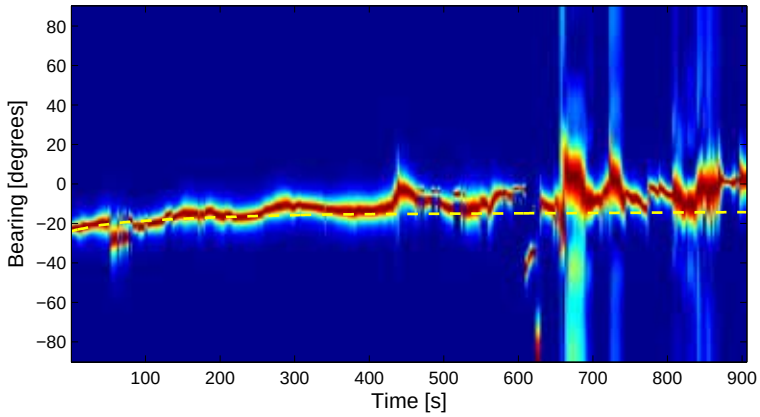

Figure 45: *Time-Bearing spectra for Ägir in Track 1 using MUSIC with the single frequency method. The SCM is recursively updated using a static* α *value,* $\alpha = 0.07$*, where the length on estimation window is set to* 1 *s. p is set to* 1.

Table 2 shows the estimated RMS, STD and bias errors for CB, MV and MUSIC in Figure 43-45.

Table 2: *RMS, STD and bias errors for Track 2 using a* 1 *s estimation window with static recursive updating of the SCM,* $\alpha = 0.06$.

	RMS, [°]	STD, [°]	Bias, [°]
CB	9.45	8.42	-4.29
MV	8.67	8.28	-2.61
MUSIC	10.05	9.08	-4.33

Track 3

Track 3 is a recording of two vessels, Ägir and Decibella, both equipped with an acoustic signal generator that emits a 200 *Hz* signal. Only the 500 first *s*, where the two vessels are most separated are used of this recording.

Figures 46-48 show the obtained Time-Bearing images for CB, MV and MUSIC using a modified version of the *mean power method*. The modification is that instead of a direct averaging of the obtained Power-Bearing spectra as described in Section 5.2, each spectra is first normalized before averaging. This is done with the purpose of trying to enhance weak sources. The SCM is recursively updated with the static updating method described in Section 5.5.1 with $\alpha = 0.1$. The estimation window has a length of 1 *s* and p is set to 2 for the MUSIC based algorithm. As a reference to the estimated bearings, the GPS signal to Ägir (plotted in yellow) and Decibella (plotted in red) are used.

As can be seen in the figures the tracking is not very satisfying in this case. For both CB and MV it is impossible to see that there are two sources present. For MUSIC it can be suspected that there are two sources present. The problem with the separation can be illustrated by trying to estimate the number of sources p by using the gradient method. This is shown in Figure 49.

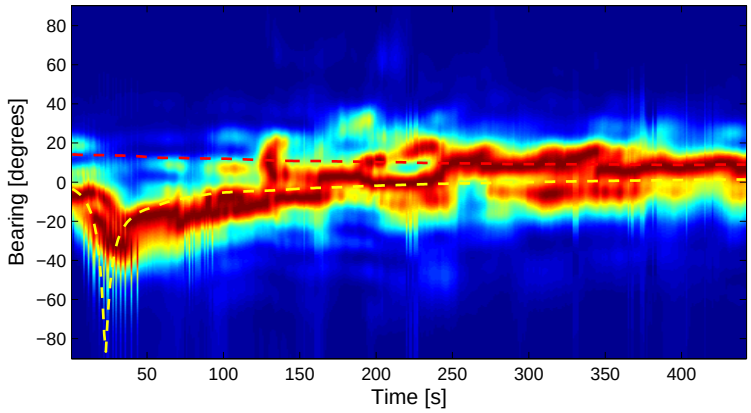

Figure 46: *Time-Bearing spectra for the tracking of Ägir and Decibella in Track 3 using CB. The SCM is recursively updated using a static α value, $\alpha = 0.1$, where the length on estimation window is set to 1 s. Used approach is a modified mean power method.*

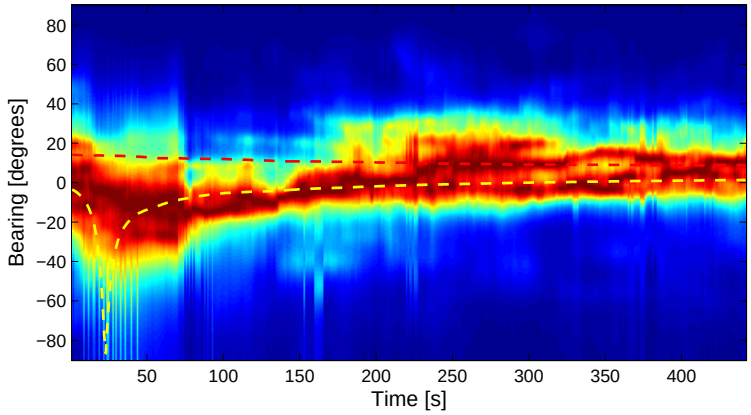

Figure 47: *Time-Bearing spectra for the tracking of Ägir and Decibella in Track 3 using MV. The SCM is recursively updated using a static α value, $\alpha = 0.1$, where the length on estimation window is set to 1 s. Used approach is a modified mean power method.*

As can be seen in the figure the gradient method is unable to estimate a true value on the number of sources p. Instead the method indicates on that there is only one source present most of the time. The problem with the lack of separation in this track can be explained first on the equal emitted 200 *Hz* signal and second on the small bearing separation, the sources are very close to each other during almost the entire recording. For CB the algorithms resolution properties set the limit. Also in theory the two sources are too closely spaced most of the time to be separated from each other. The MV algorithm should in theory be able to separate the two vessels in this case, but it fails. The MV algorithm suffers from a broad main lobe and high side lobe levels that can explain this. MUSIC should in theory easily resolve the two sources. It does to some extent, but the result is not convincing. If the sources more clearly had been separated in bearing it would maybe have been possible to resolve them even if the frequency was the same.

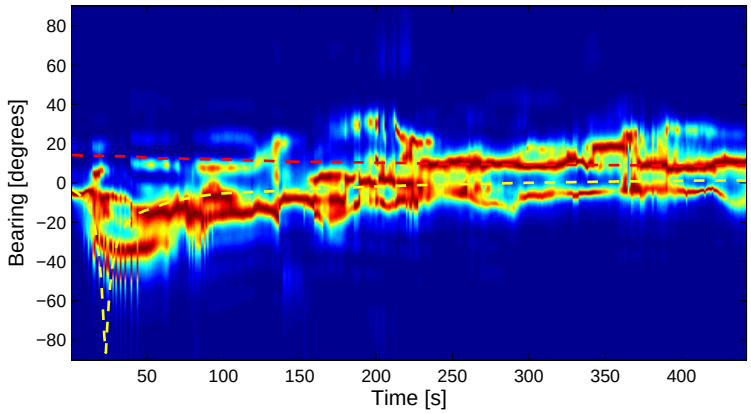

Figure 48: *Time-Bearing spectra for the tracking of Ägir and Decibella in Track 3 using MUSIC. The SCM is recursively updated using a static α value, $\alpha = 0.1$, where the length on estimation window is set to 1 s. p is set to 2. Used approach is a modified mean power method.*

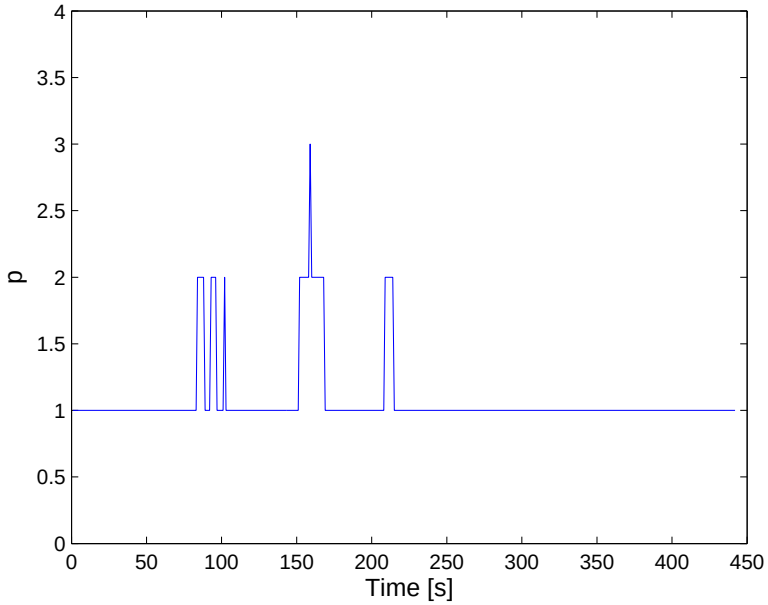

Figure 49: *Estimated number of sources p for Track 3 using the gradient method.*

One approach to solve this problem is to use the signature of the vessels instead. A part of Ägir's signature is already known from *Track 1* and *Track 2*. From the spectrogram for *Track 3* in Figure 19 (Section 4) it can be seen that the frequencies that originates from Ägir is prominent during most of the recording. By steering towards these frequencies the tracking of Ägir should be possible without interference from Decibella. The frequencies created by Decibella are most significant in the interval from 200 *Hz* and upwards. They are rather strong in the beginning of the recording when Decibella is close to the array and the separation between the vessels is

as largest. When Decibella moves away from the array the amplitude of the frequencies are reduced, so that they drown in the stronger signal from Ägir and the strong emitted 200 *Hz* signal. This makes it impossible to track Decibella from these frequencies when Ägir is present.

5.7 Resolution

As explained in Section 3.2-3.4 one of the key reasons for using other methods than CB is that CB suffers from poor resolution properties. The resolution can in theory be improved by using the high-resolution methods MV or MUSIC, which was shown in Figure 6, 7 and 8. In real measurements this is not certain. The resolution properties of both MV and MUSIC are strongly dependent on that the noise can be considered white. This is not the case in these measurements.

The resolution is for all three methods dependent on the length L of the array aperture. According to [18] a good approximation is to say that the resolution will be a function of the effective array length. The effective array length is a function of the DOA θ, which is shown in Figure 50.

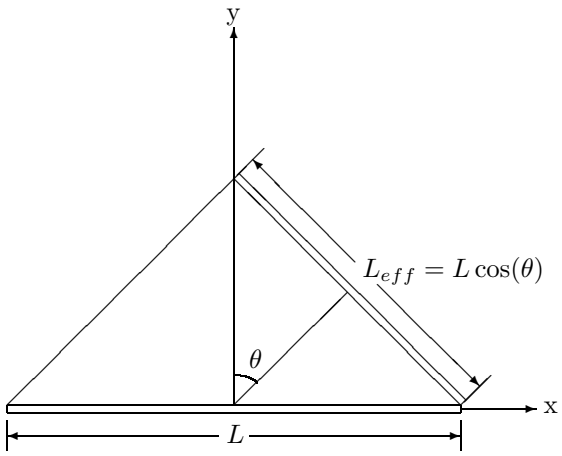

Figure 50: *Effective array length as a function of the DOA.*

According to the figure, the effective array length L_{eff} decreases when the source moves away from Broad Side of the array. When the effective array length decreases the main lobe becomes broader (see Figure 51) and the resolution decreases. The main lobes are estimated for a 200 *Hz* signal. The width of the main lobe is strongly affected by the frequency of the signal, where low frequencies gives broader main lobes than higher frequencies.

Figure 52 shows the measured resolution and the theoretical resolution for *Track 1* as a function of the DOA θ for a 1 *s* estimation window without recursive updating ($\alpha = 1$). The theoretical resolutions are estimated for a signal with frequency 200 *Hz*. The resolution measurement is limited to the interval $0 - 2200$ *s*. The resolution is obtained for each method by first normalizing the power P and then calculating the width of the lobe at half the maximum value (the 3 *dB* bandwidth).

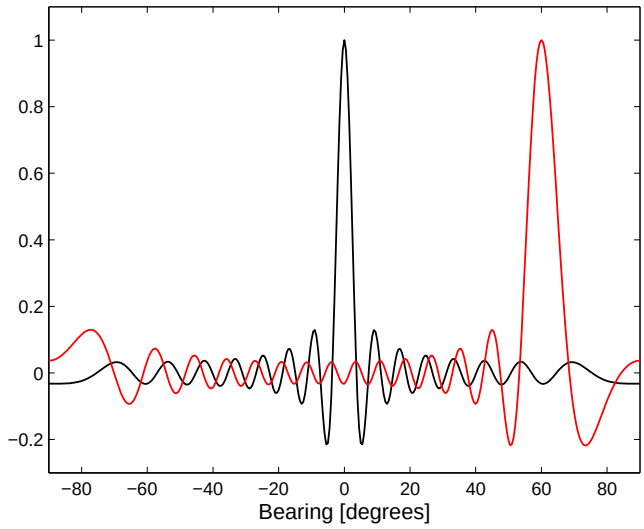

Figure 51: *The black curve represents the resolution properties for CB when the source is at the broad side of the array ($\theta = 0°$). The red curve shows the situation for CB when the DOA θ is $60°$. The main lobe for the red curve is broader than main lobe for the blue curve, which shows that the resolution decreases when the source moves towards the End Fire of the array.*

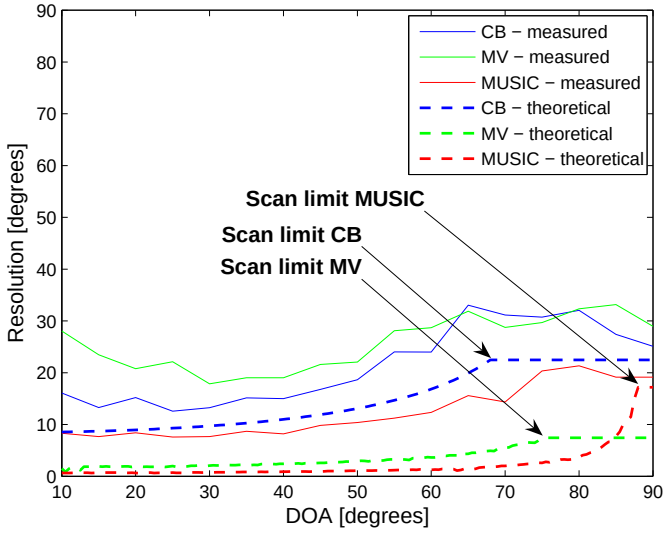

Figure 52: *Theoretical and measured resolution for CB, MV and MUSIC for Track 1. The length of the estimation window is* 1 *s and no recursive updating of the SCM is used. The theoretical curves are estimated for* 200 *Hz.*

As can be seen in the figure the measured resolution is improved for the described high-resolution MUSIC algorithm (red line) compared with the measured resolution for the CB

algorithm (blue line), as in theory. But the measured improvement does not agree with the theoretical improvement. For MV (green line) the measured resolution is decreased compared with CB. The reason for this poor resolution improvement for MUSIC and the decreased resolution for MV is probably dependent on that these high-resolution algorithms are more sensitive to multipath propagation and other ambient disturbances than the more robust CB algorithm. For MV the inverse of the SCM can also influence on the resolution results. The measured resolution is not so much affected by the recursive updating and will almost be the same for all of the evaluated values on α.

For each algorithm the theoretical resolution has a limitation point, a maximum usable DOA that can be resolved. Beyond this maximum point a source can not be resolved unambiguously and the theoretical resolution can not be used for any reliable measurements. An explanation to this is according to [18] that the main lobe becomes too wide which results in that one side of the main lobe has no half-power point, and therefore no 3 dB bandwidth can be estimated. The limit depends on the length of the array and increases with the array length. The limit is referred to as the *scan limit*. The *scan limit* is different for each algorithm, worst for CB and best for MUSIC. It is marked with an arrow for each algorithm in Figure 52, where the interval beyond the limitation point is made flat.

6 Error Discussion

In real applications it is natural to think that there are different types of error sources that affects the bearing estimation. With the knowledge about the error sources it is easier to evaluate the bearing algorithms performance and which error rate to expect. Some of these different error sources are briefly described below.

6.1 Disturbances

In every real application there are always some disturbances from the channel that will influence on the bearing performance, e.g. multipath propagation, other vessels, imperfect sensors or thermal noise. With Multipath propagation means that the signal bounces against e.g. the surface or/and the sea bed. This leads to that the signal will propagate different ways toward the ULA and will at the sensors in the array appear as multiple sound sources. The multipath propagation has more influence on the bearing performance at large ranges than at short ranges (multipath propagation is a greater source of errors for a vertical array).

All these disturbances break the assumptions about isotropic noise made in Section 2.3.2. A good model would require considerations of the disturbances which is very hard to predict and implement.

6.2 Hydro Acoustic Properties

The wave propagation media is assumed to be homogeneous and non-dispersive, so that the waves arriving at the array can be considered planar. The media is actually dispersive which can introduce errors in form of incorrect correlation between the M sensors in the array which results in incorrect bearing information in the SCM. Also, the speed of the sound c and the frequency f can be strongly affected by a dispersive media, which can create bias in the steering vector (see Eq. 14 in Section 3.2). The speed of sound c can be described as [19]

$$c = 1448.96 + 4.591T - 0.05304T^2 + 0.0002374t^3 + 1.34(S-35) + 0.0163D -$$
$$-0.01025(S-35)T + 1.675 \cdot 10^{-7}D^2 - 7.139 \cdot 10^{-13}TD^3$$

where T is the temperature in Celsius degrees, S is the saltinity in parts per million and D is the depth in meters.

6.3 Errors in the ULA

The linear array is assumed to have a uniform sensor spacing with omni-directional sensors. The array is assumed to be stretched out along the sea bed and the depth of each sensor element equal. An error in the array configuration regarding sensor spacing introduces bias to the steering vector, which will affect the bearing information in the SCM, and decrease the bearing performance. The sensors can be misplaced in the vertical direction and/or the horizontal direction. If, for example, there is a linear elevation difference between the sensors this will yield a decreased effective array length which decreases the bearing resolution. Horizontal direction means an error in the physical array configuration regarding the sensor spacing. The accuracy in the sensor spacing is assumed to be approximately 0.1 m. If the array is not fully stretched out horizontally, this have the same effect as unequal sensor spacing. Also, the sensors are not perfectly omni-directional which will increase the error when the source moves from the Broad Side of the array towards the End Fire of the array.

6.4 Geometric Errors

The bearing performance for the ULA is as best when the source is in the vicinity of the array Broad Side and as worst when the source is close to the End Fire of the array. When the source moves away from the Broad Side of the array towards the array End Fire the effective array length will be decreased, which will make the main lobe broader. Therefore, the error will be larger for larger angles. The error in the DOA can be described as

$$\sigma^2_{direction} = \sigma^2_{timedelay} \left[\frac{c}{d} \sin(\theta) \right]$$

where $\sigma_{timedelay}$ is the time delay error, c is the speed of sound in water, d is the sensor spacing and θ is the DOA.

7 Conclusions

This chapter summarizes the findings in this thesis and some suggestions for future improvements.

7.1 Findings

The bearing accuracy has been shown to be dependent on the length of the estimation window, where a longer estimation window yields a better bearing performance, see Section 5.4. This is because the SCM approaches the true value when more signal data are used. At some point the improvement in bearing performance stabilizes around a constant performance, regardless of the estimation window. This asymptotic effect is presumably due to that for longer estimation windows the signal can not be considered stationary. A major drawback with using long estimation windows is that the time-lagging and the computational time becomes larger.

The bearing performance has been shown to be significantly improved by recursive updating of the SCM, see Section 5.5. The optimal performance has been shown to be the same independent on the length of the estimation window. The updating constant α depends on the length of the estimation window. It will be smaller for a shorter estimation window and larger for a longer estimation window. This opens up the possibility to use shorter estimation windows together with small α values and thereby avoid long time-lagging and long computational time, and still obtain high bearing performance.

Both recursive updating methods evaluated in this thesis yield approximately the same bearing performance for CB and MUSIC when the source has a strong signal. For MV the static updating method (Section 5.5.1) has better performance than the SNR dependent method (Section 5.5.2). When the signal is weaker, both methods yields approximately the same bearing performance. Still, the static updating method is the recommended method to use, because of its simplicity to implement combined with sufficient bearing performance.

Three different approaches have been used and evaluated in the analysis of the bearing performance: the *single frequency method*, the *maximum peak method* and the *mean power method* (see Section 5.2). Both the *single frequency method* and the *mean power method* has been shown to yield a good bearing performance. The first is the best to use when the source has one dominating signal i.e. the source is of narrowband character. The second is better when the source has several equally strong signals i.e. the source has a more broadband character. The *maximum peak method* is the least good of the three evaluated methods under the present conditions.

Conventional Beamforming has been shown to be very robust against the uncertainties in the assumed model. Keeping its limitations in mind, the algorithm gives reasonable bearing performance if the vessel had signal generator or not. One drawback is that it inability to resolve two closely spaced sources. The inability can be dependent on that the sources emit a signal with the same frequency which complicates the separation.

The Minimum Variance based method, in its present design, has been shown to have poor bearing performance. Its theoretical superior resolution compared with Conventional Beamforming does not come to its full rights under the present conditions in these practical measurements. The poor performance may be due to the algorithm being strongly affected by e.g. multipath propagation or coloured noise. In its present design, the Minimum Variance method is not a recommended algorithm to use.

The MUSIC based method has been shown to possess the best bearing performance of all

three evaluated methods. It has the best resolution properties, and it is able to separate two closely spaced sources, even if both sources emit a signal with the same frequency. One drawback with the algorithm is that the practical measured resolution is much worse than the theoretically resolution. But it is still two times better than the measured resolution for Conventional Beamforming. The degraded resolution might depend on poor statistical properties and multipath propagation. From the measurements it has been shown that using a too large value on the factor p does not affect the performance noticeably.

The gradient method used to estimate the number of sources p has been shown to be a good estimator in the case of one source present, with or without signal generator, but very bad when there is two sources present, both with signal generators emitting the same frequency. This can be dependent on that the method is either insufficient or that the task is very hard to accomplish.

7.2 Suggestions to Future Improvements

Finally, some suggestions to future improvements,

- Using the Welch averaging method and/or some sort of pre-processing to lower the variance and obtain better estimates of the SCM. Each block must at least have a length that is equivalent to two periods of signal data.
- Using an adaptive method to decide the length on the estimation windows, from the stationarity time of the signal or the noise. See [12], Chapter 3, for further information about the stationarity time of the noise.
- Using a more adaptive method to recursively update the SCM dependent on the SNR changes.
- Using adaptive beamforming instead of Conventional Beamforming to obtain better resolution properties. This method can perhaps have better properties than MUSIC have under the conditions of the present measurements.
- Remove "incorrect" bearings, i.e. bearings that differ too much from the previous bearing to be considered as a true movement of the source. The "new" bearing can either be chosen from the estimated power-bearing spectra by taking the highest peak that fulfils the criterion or it can be predicted by using the trend from the previous estimated bearings.
- Using a steering vector with non-uniformly separated looking directions. Instead, the directions are adapted to the broadening of the main beam, i.e. smaller separation between the direction close to broad side and larger separation close to end fire.
- Improve the MV algorithms reliability by using diagonal loading of the SCM to prevent singularity, and by that means make sure that the inverse to the SCM exists.

Acknowledgements

This Master thesis work has been carried out between September 2005 and March 2006 at the Swedish Defence Research Agency FOI in Kista.

First of all, I would like to thank my supervisors at FOI, Ron Lennartsson, Leif Persson and Mika Levonen, for allowing me to do my thesis at FOI. Their help and advice have been very useful and helped me to succeed with the thesis. I also like to thank Magnus Lundberg, Eva Dalberg and all other people at FOI for their support during the time at FOI. Finally, I would like to thank my supervisor at KTH, Magnus Jansson, for his support and help.

References

[1] Anderson, E.; Bai, Z.; Bischof, C.; Blackford, S.; Demmel, J.; Dongarra, J.; Du Croz, J.; Greenbaum, A.; Hammarling, S.; McKenney, A.; Sorensen, D. (1999), *LAPACK User's Guide* (*http : //www.netlib.org/lapack/lug/lapack_lug.html*). 3^{ed}. Philadelphia: SIAM. ISBN 0-89871-447-8.

[2] Cox, H. (1973). Resolving Power and Sensitivity to Mismatch of Optimum Array Processors. In: *Journal Acoustical Society of America*. Vol. 54, No. 3, pp. 771-785.

[3] Crona, Lennart; Dalberg, Eva; Lennartsson, Ron; Lundqvist, Björn; Morén, Per; Persson, Leif; Söderberg, Per (2004). *An Experiment on Passive Multi-Sensor Underwater Surveillance*. Stockholm: FOI Systems Technology. FOI-R–1336–SE. ISSN 1650-1942.

[4] Gåfvels, Lennart; Persson, Leif; Tenstam, Johan (1989). *Högupplösande Riktningsmätning med Mångelementsantenn*. Technical report MTA E0070 Teleplan (in swedish).

[5] Gaucher, Damien; Gervaise, Cédric; Jourdain, Geneviève (2004). Feasibility of Passive Ocean Acoustic Tomography in Shallow Water Context: Optimal Design of Experiments. In: *Proceedings of the Seventh European Conference on Underwater Acoustics*, Delft (Netherlands), July 5-8 2004.

[6] Golub, Gene H.; Van Loan, Charles F. (1996). *Matrix Computations*. 3^{ed}. London: The Johns Hopkins Press Ltd. ISBN 0-8018-5414-8.

[7] Göransson, Bo (1992). *Parameter Estimation from Hydroacoustic Sensor Array Data: Experimental Results*. Linköping: Linköping Institute of Technology.

[8] Haykin, Simon (1991). *Adaptive Filter Theory*. New Jersey: Prentice-Hall Inc. ISBN 0-13-013236-5.

[9] Johnson, Don H (1982). The Application of Spectral Estimation Methods to Bearing Estimation Problems. In: *Proceedings of the IEEE*. Vol. 70, No. 9, pp. 1018-1028. New York: IEEE Inc. ISSN 1018-9219.

[10] Johnson, Don H.; DeGraaf, Stuart R. (1986). Improving the Resolution of Bearing in Passive Sonar Arrays by Eigenvalue Analysis. In: *Modern Spectrum Analysis, II*. pp. 268-277. New York: IEEE Inc. ISBN 0-87942-203-3.

[11] Kopka, Helmut; Daly, Patrick W. (1999). *A Guide to LATEX*. 3^{ed}. Harlow (England): Addison Wesley Longman Limited. ISBN 0-201-39825-7.

[12] Levonen, Mika (2005). *Sonar Data Characterisation and Analysis*. PhD thesis, The University of Edinburgh.

[13] Lindquist, Erik (1995). *Kurtosis Estimation in the Frequency Domain used in Multipath Detection*. Linköping: Linköping Institute of Technology. ISSN 1104-9154.

[14] Prabhakar, S. Naidu (2001). *Sensor Array Signal Processing*. USA: CRC Press LLC. ISBN 0-8493-1195-0.

[15] Proakis, John G.; Manolakis, Dimitris G. (1996). *Digital Signal Processing: Principles, Algorithms and Applications*. 3^{ed}. New Jersey: Prentice-Hall Inc. ISBN 0-13-394289-9.

[16] Stoica, Petre; Moses, Randolph L. (1997). Spatial Methods In: *Introduction to Spectral Analysis*. pp. 221-254. New Jersey: Prentice-Hall Inc. ISBN 0-13-258419-0.

[17] Tenstam, Johan (1989). *High-Resolution Direction of Arrival Estimation by means of Sensor Array Processing*. Uppsala: Uppsala University. ISSN 0346-8887.

[18] van Trees, Harry L. (2002). *Optimum Array Processing: Part IV of Detection, Estimation and Modulation Theory*. pp. 42-89. New York: John Wiley and Sons Inc. ISBN 0-471-09390-4.

[19] Urick, Robert J. (1982). *Sound Propagation in the Sea*. Los Altos (USA): Peninsula Publishing. ISBN 0-932146-08-2.